UCLouvain

École polytechnique de Louvain

Development of a reference one-dimensional pyrolysis experiment

Author: **Dimitri GREVESSE**
Supervisor: **Hervé JEANMART**
Readers: **Arnaud ROUANET, Julien BLONDEAU, Matthieu DUPONCHEEL**
Academic year 2020–2021
Master [120] in Electro-mechanical Engineering

Abstract

The comparison of the results of two scientific communities working on pyrolysis but in different application areas, i.e. biomass conversion and protective heat shields, is envisaged. For this purpose, a pyrolysis test bench is set up for a comparative thermogravimetric analysis (TGA) experiment. Measurements of temperature distribution and mass loss are carried out on large cylindrical samples of Beech wood during slow pyrolysis in an inert atmosphere from ambiant temperature to 650 [°C] at a heating rate of 40 [°C/min]. The pyrolysis proceeds from the bottom to the top of the cylinder and is considered to be one-dimensional. Devolatilization does not compare well to models and increases towards the end of the mass loss, due to the splitting of the sample. There is a problem with the design of the heat source which compromises the quality of the experimental results.

Remerciements

Ce mémoire marque la fin d'un cycle d'étude dont les objectifs et le cadre m'ont apporté beaucoup de choses. Notamment, un savoir partagé, accumulé au fil des siècles et dont la beauté se retrouve dans la déclinaison des mathématiques à travers la physique, ainsi qu'une méthode critique d'évaluation des connaissances extractibles à partir d'observations données. Dans ce cadre, je remercie Jérémy De Visscher pour le temps qu'il a consacré avec moi dans la plupart de mes travaux d'études et ce mémoire ainsi que pour la qualité de son organisation. Je remercie mes parents qui m'ont aidé à me motiver dans la rédaction du mémoire, ainsi que tous ceux qui ont bien voulu relire ce travail et me donner leur feedback afin que je puisse l'améliorer. Je remercie Hervé Jeanmart pour sa supervision du travail tout au long de l'année. Je remercie Arnaud Rouanet pour sa présence au moment critique, pour sa manière d'avoir guidé ma méthode d'analyses des résultats, et pour son accessibilité. Je remercie tous ceux qui ont rendu possible la réalisation technique et administrative du banc d'essai. Je remercie donc Arnaud Lion pour la réalisation des plans, Frank Hesbois pour l'instrumentation et les nombreuses réparations faites entre les expériences, Hervé Delafontaine et Julien Vervotte pour les soudures et l'assemblage, Vincent Musette pour l'usinage des pièces spécifiques, Antoine Bietlot pour le prêt du data logger des thermocouples et pour l'installation de son programme de collecte des mesures sur l'ordinateur du laboratoire, Philippe Eliaers, Pascal Carlier et Luc Wautier pour la validation de l'analyse de risque et du prototype d'expérience. Finalement, je remercie le jury de ce mémoire, c'est-à-dire Hervé Jeanmart, Arnaud Rouanet, Matthieu Duponcheel et Julien Blondeau pour avoir accepté d'en faire partie, et prendre le temps de vérifier la qualité de mon travail.

Contents

Introduction

Biomass conversion energetic issues Our modern societies cannot live without energies and the demand is constantly increasing. The recent concern about carbon dioxide emissions and the increasing difficulty to extract fossil energies has brought a lot of interest to the renewable energy sources. Among them, biomass hold a very particular role as it can be stored easily and does not suffer from intermittency like sun or wind power. It is also a good energy vector that can be transported over long distance unlike the hydro or geothermal power. The petroleum products are currently providing 93% of the energy linked to the global transport[2] and the only alternative to fossil fuel used in internal combustion engines is biofuels. The exploitation of biomass residues is particularly relevant in the case of agricultural activity where the intensive production of a plant generate huge amounts of waste and by-products or in the case of municipal solid waste, industrial waste or wood waste [12]. Part of the forests can even be harvested to avoid forest fires. Instead of burning directly into the atmosphere, the wood is converted into biofuel and later into useful work [36]. In this frame, pyrolysis is a thermochemical process of importance that converts the low energy density biomass feedstock to lighter, easier to handle, and denser energy carrier. [31] This devolatilization is a key step for the thermochemical conversion routes such as gasification and combustion. Although, it may also be an independent process to produce liquid biofuel. Biomass conversion is therefore an area full of opportunities that should be explored as it could solve many of the problems of today and tomorrow.

Scope of this thesis This work is a project initiated by Hervé Jeanmart, developed last year by a pair of students, Gilles Mottiat and Julien Benoit, during their master thesis and extended this year at the same occasion by two students, Jérémy De Visscher and Dimitri Grevesse, with the help of Arnaud Rouanet as assistant. The intention is to set up a pyrolysis test bench at the UCLouvain to develop an experiment that brings together and compares the work done in data collection and modelling of two scientific communities both working on a particular field of application of pyrolysis. On the one hand there is biomass conversion, the issues of which have been detailed above, and on the other hand there are thermal protection shields (TPS) in the aerospace field. These two communities have not yet compared their formalism and could help each other for better results. The test bench will also be used for didactic purposes.

Outline of the work In the first chapter, the phenomenon of pyrolysis is presented in the specific context of lignocellulosic biomass conversion. In chapter 2, the main reactors, models and results from the relevant scientific literature that focus on large particles are presented. Then, the final reactor design, as well as the history of its assembly is presented in chapter 3. After that, the results of the experiment are analyzed in chapter 4 using the knowledge from chapters 1 and 2 and a discussion about the problems encountered in the experiments is held. Finally, improvements to the test bench and future experiments are considered in the last chapter.

Chapter 1

Pyrolysis mechanism

After this contextualisation, the motivations to study pyrolysis is addressed, as well as the wood specificity and pyrolysis phenomenology, in order to facilitate the reader understanding of the experimental scientific results that will be presented in the next chapter.

1.1 Motivations

Biomass has the disadvantage of having a variable composition and a more complex structure than hydrocarbons. In order to achieve economic viability, it is therefore necessary to carry out studies on the understanding of the phenomenon to make a better use of this energy [20]. At the industrial level, the study of thermally thick particles would help to simulate properly the reactor performances, understand pollutant evolution, and determine strategies for effective control in combustion, gasification and pyrolysis in fixed beds [27, 21]. For example in the case of gasification, CO and H2 are the desired products and it is important to understand the pyrolysis reactions that promote their production [27]. In the field of fire safety, the study of pyrolysis provides a better understanding of the mechanisms behind devastating fires [15] and in the aerospace field, this guides the design of thermal protection shields suitable for bodies entering an atmosphere. But pyrolysis products are also useful in many applications, the pyrolysis oil can be upgraded to biofuel or converted to a suitable chemical product [12]. The char can also be processed and used as a reagent in the steel, chemical and pharmaceutical industries. In addition, it can be used as an adsorption agent for pollutants and it is expected that the use of char and its properties will increase in various fields in the next decade. [28, 12].

1.2 Wood fuel

1.2.1 Wood composition

Wood is a lignocellulosic biomass that transforms trough pyrolysis into second generation biofuels [2]. It is composed of 3 main polymers that make up its structure, namely hemicellulose (25-35%), cellulose (40-50%), lignin (15-20%) [12]. Hemicellulose is decomposing between 200 and 375 [°C], cellulose is decomposing, between 275 and 380 [°C], and lignin is decomposing gradually between 180 and 550 [°C] [21] (figure 1.1).

Its composition can also be characterized according to its thermal degradation, through proximate analysis where the fraction of moisture is evaporated, followed by the devolatilization of volatile matter and finally the fixed char is burned with oxygen (figure 1.2). The residual solid is called the extractives, i.e. the ashes content. This characterization is important because even a low concentration of ashes and impurities

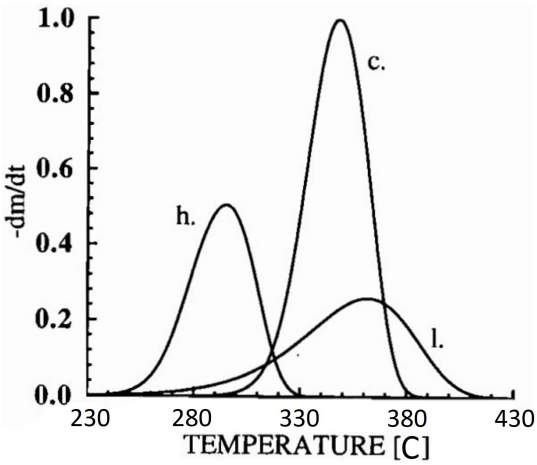

Figure 1.1: Mass loss rate from Miller and Bellan model predicition with 10 [K/min] for cellulose (c),hemicellulose (h) and lignin (l).

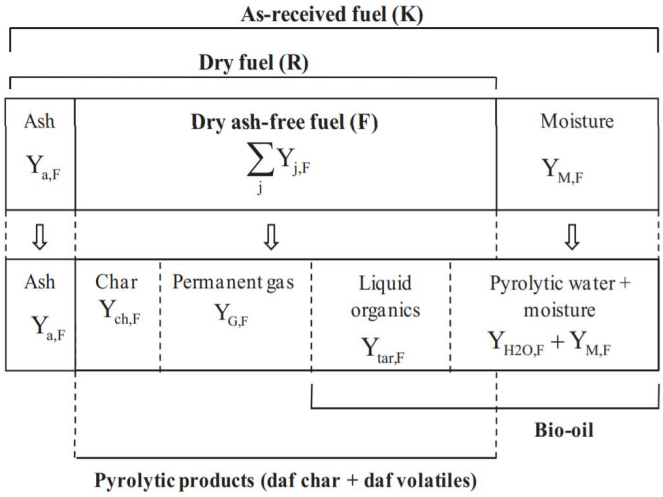

Figure 1.2: Biomass composition from proximate analysis

may have a catalyzing or inhibiting effect on biomass devolatilization [29]. A third representation of the wood composition is enabled by the ultimate analysis that describe the composition in terms of C,H,O,N atoms. The result of an ultimate analysis is usually more comprehensive than of a proximate analysis.

Unfortunately, wood is difficult to handle because its composition as well as many parameters change from specie to specie and from one feedstock to another. To reduce fuel variability, the raw biomass samples were taken on the same piece of wood and the chosen specie is beech wood because its thermal degradation is one of the most studied in the literature [15, 17, 13, 43, 10, 14, 30, 19, 2].

1.2.2 Moisture and drying

Water is present in 3 physical states in a piece of wood: liquid or free water, water vapor and bound water. The liquid water and water vapor are at thermodynamic equilibrium at rest and are free from flowing into the porous matrix of the wood. This water content can be removed from the wood by drying it at around 100[°C]. The bound water, however, is chemically linked to the wood by hydrogen bounds but can yet be released during the pyrolysis and is also called pyrolytic water (figure 1.2).

1.3 Phenomenology

The pyrolysis is formally the chemical degradation process of an organic solid subjected to a thermal flow in the absence of oxygen. The feedstock is usually broken down into non-condensable gases, condensable volatiles also called tars and a residual solid. However, many other effects occur simultaneously and are described in the following sections.

1.3.1 Small and large scale

On a small scale, pyrolysis is the set of reactions that take place under the action of a uniform increase in temperature and the dynamics of the phenomenon is limited either by the kinetics of chemical reactions or by the external heat transfer. In this set of multiple reactions, some are in competition with others, some are endo- or exothermic and they are difficult to isolate from each other to identify them precisely.

On a large scale, the phenomenon is more complex than on a small scale because the temperature increase is no longer uniform in the medium and internal mass and heat transfers intervene as elements limiting the dynamics of the phenomenon. Thus the shape of the particle influence also dynamic of the pyrolysis [25]. The internal transfer cannot be neglected compared to the external transfer and the medium is said to be thermally thick. It is the case for centimetric particles, where the Biot number is higher than 1 [38]. Other macroscopic effects then emerge and are detailed in the following sections.

1.3.2 Heat and mass transfer

On a large scale, the heat comes from the surface and penetrates towards the center of the particle. In this direction, 3 distinct zones appear in the following order: a char zone, a pyrolysis front, and a virgin zone. The char zone extends from the surface and corresponds to the biomass that has already been pyrolyzed by the external heat, then the pyrolysis front is the zone where devolatilization occurs, and finally the virgin zone is the area closer to the center that has not yet reacted (figure 1.3).
For sufficiently slow pyrolysis, a drying front takes place between the virgin zone and the pyrolysis front as the wood slowly evaporates its free water before rising in temperature and starting to pyrolyze [19, 23]. In other words, as the devolatilization occurs, hot gases expelled from the pyrolysis front pass through the char porous matrix to the outside and mass and heat transfer phenomena occur throughout the particle. Radiation, conduction, and convection occurs everywhere in the medium.

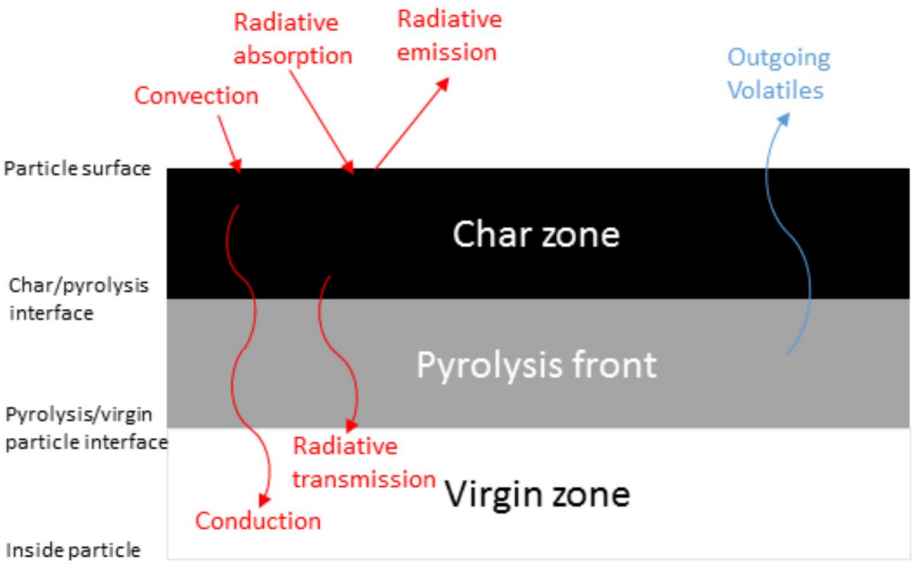

Figure 1.3: Pyrolysis macroscopic phenomenon

1.3.3 Secondary reactions

The chemical reactions during pyrolysis are classified into two groups: The primary reactions, or devolatilization reactions whose reactants are coming from direct degradation of the biomass and secondary reactions whose reactants are the products of primary reactions. They consist mainly of reactions of reforming, cracking, oxydation, water-gas shift, dehydration, polymerization and gasification [17]. Temperature and residence time have a strong effect on the final products composition, as these parameters control the intensity of secondary reactions.

1.3.4 Internal pressure generation

Gas production in the wood generates a pressure gradient and therefore an outward mass flow in the particle. If the heating is more intense, the gas production and the internal pressure increase. If the coal is less porous, the internal pressure increases further. The pressure peak is caused rather by small permeability than by rapid gas generation and it appears at the end of the pyrolysis when the gas have to travel a longer path trough the char [36].

1.3.5 Shrinking

During the pyrolysis process, anisotropic shrinkage is observed on the particle and can reach up to 40% in the transversal direction and 25% in the longitudinal direction [2]. As the solid structure is constantly deformed and weakened, cracks are forming and can lead to the splitting of the sample. This behavior is also dependant on the type of biomass [15]. At high heating rates, huge cracks appears in hardwoods on the contrary of softwoods. Much remains to be discovered about the mechanisms that create cracks in a sample during pyrolysis, but it is known that internal pressure plays an important role [36].

1.3.6 Products yield

There exists a whole spectrum of pyrolysis heating conditions, the extreme of which are fast and slow pyrolysis. The change in heating rate, temperature and residence times is strongly influencing the products yields and the different types of pyrolysis are explained below.
Slow pyrolysis of biomass is conducted at low heating rates and long residence times [13]. The liquid yield is then at the lowest and the wanted product is usually the residual torrefied or carbonized solid. The increasing pyrolysis temperature implies a higher gas yield, lower char yield and higher carbon content in the char. Nevertheless, this temperature remains low compared to what is found in gasifiers [31]. Longer residence time is a solution to convert even further the liquid yield into gas [12, 13, 42].
On the other hand, fast pyrolysis of biomass is conducted at high heating rates and slow residences times, when the desired product is bio-oil [3, 13, 44]. However, for large particles the volatiles released do not leave the particle immediately and interact with the char, undergoing secondary reactions [41]. For this reason, fast pyrolysis is done usually on small particle and primary products are quickly cooled down to condensate bio-oil. Fast pyrolysis heating rate should be around 100 K/min to obtain an optimal liquid yield, up to 75% [32, 4, 5].
Intermediate pyrolysis is a mixture of the characteristics of slow and fast pyrolysis whose liquid, solid and gas yields are respectively 50%,25% and 25% [5].

Chapter 2

Particle pyrolysis : state of the art

To give a context to this experiment in relation to what has already been done in the scientific world, a variety of reactors, models and results of large particle pyrolysis experiments are presented in this chapter. In the scientific literature, there are different types of pyrolysis experiments. This study deals with a TGA experiment and there is no need to compare it to anything other than a TGA experiment. Note that the other types of experiments are called drop tube reactor (DTR) experiment [30] and electrode heating experiment [11]. In a DTR experiment, small particles are dropped into a hot tube, undergoing a very high heat flux. The residence time is determined by the length of the tube and the results are more difficult to extract from the data collected. Electrode heating experiment are carried out to reach very high heating rates in small zones but have also some disadvantages.
In the first section, two reactors for large particles are presented, to give a sense of different potential designs for similar experiments. Then, different robust models are presented to help the understanding of the effects underlying the experimental observations. Finally, results of parametric studies on TGA are shown and commented, to deepen the understanding of the heating conditions effect on the pyrolysis.

2.1 Large particle pyrolysis reactors

2.1.1 Vertical tube furnace reactor

The reactor developed in G. Gauthier 2013 [2] is a vertical tube furnace where a large cylindrical particle of 20mm diameter and 30mm height is placed.

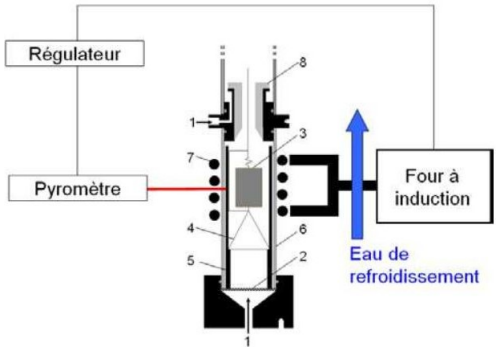

Figure 2.1: Vertical tube furnace reactor

The reactor is surrounded by a transparent quartz tube. An inner metallic tube is heated by induction with the help of external coils. The oven maximum power is 12kW with a temperature increase speed

of 500$[C/s]$ The temperature at the hottest point is measured with an infrared pyrometer with laser sighting. It is then controlled with a PID regulator to reach the desired temperature setpoint. Nitrogen is flowing upward at 2$[NL/min]$ in order to prevent fouling on the inner walls of the furnace while keeping a concentration of volatiles products that match the sensitivity of the gas analysis cells. The advantages are that the temperature measurements and energy source are contactless and this makes it much easier to use the device.

2.1.2 Xenon Arc Lamp Reactor

This reactor was developped by M. Gronli 1996 [9] and inspired form the work of Krieger-Brockett and co-workers [6, 7, 8].

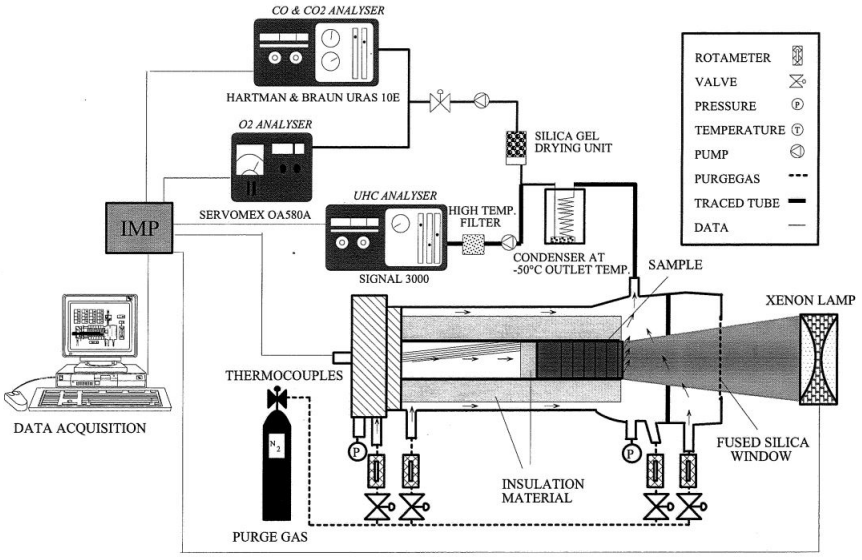

Figure 2.2: Xenon arc lamp reactor

It has a horizontal tubular shape where a large cylindrical particle of 20 [mm] diameter and 30 [mm] length is placed. The reactor is composed of an outer tube that acts as a wall and an inner tube where the sample is tightly fitted. One face is subjected to the heat flux while the others walls are being insulated, and it can be considered as 1-dimensional heating. The heat flux is provided remotely by a Xenon arc lamp whose energy beam passes through a fused silica window. Only 10% of the energy transmitted is dissipated in the window. A heat flux of 80 or 130$[kW/m^2]$ is applied directly on the wood sample and the temperature is controlled with the help of thermocouples inside the sample and a heat flux meter.

2.2 Large particle pyrolysis models

2.2.1 Kinetic models

Kinetic modelling is as very complex task and there still no consensus concerning the kinetics of wood pyrolysis [9]. There are many kinetic models in the literature, each representing a way of approximating the reality of the chemical interactions over time by lumping reactions and chemical species into a small number of groups. The number of groups of species and groups of reactions can range from 4 [43] to more than 15 [36, 27], depending on the complexity of the model. For simplicity, all the reactions are often considered as first order reactions. The rate constant "k" of each reaction is given by the Arrhenius

equation :

$$k = Ae^{\frac{-E}{RT}} \tag{2.1}$$

Where A is the frequency factor, E the activation energy, R the universal gas constant and T the temperature.
The kinetic parameters of primary reactions are estimated trough TGA with very small particle and slow heating rate, between 20 and 40 [°C/min] [37, 39]. In these conditions, ranging from 1 to about 100 [°C/min], the rate of heat transfer to and within the particle is very fast, as compared with the reaction rate, and pure kinetic control is achieved (Bi << 1 and Py' >> 1) [38, 19]. The results are then available in the literature for further research.
The kinetic parameters of secondary reactions are more difficult to determine as they depend on wood specie, heating rate, temperature, and mass transfer conditions. As these rates are not available in the literature, they need to be adjusted according to the experience thanks to a parametric study on a case-by-case basis [9].

Single component model

In this simple model, we consider biomass as a single primary component that decomposes into pyrolysis products [43]. There may be more than one transformation before the final products and this is called a multi-step model. There also may be more than one reaction for an initial specie and this is called a competitive model. An example of multi-step and competitive network of reactions is represented on figure (2.3) :

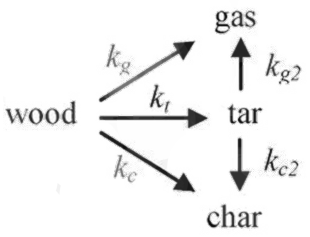

Figure 2.3: Caption

Multi-component model

This model is simply the superposition of several single component models with little interaction between them and cellulose, hemicellulose and lignin are usually considered as primary components for each independent reaction network [16, 27]. Biomass is often characterised either by its composition as lignocellulosic material or by its composition in terms of C, O, N and H atoms. This makes the multi-component representation very flexible and adaptable for a large number of biomass types whose composition are known in the scientific research [22]. Moreover, a scientific method was proposed by Cuoci et al. [40] to estimate the lignocellulosic composition of the biomass, in the case where only an ultimate analysis is available.

Chemical structure model

These are more elaborate models that defines the biomass as a chemical structure more than a sum of basic elements. It is more flexible and reliable but also more complicated to implement and use [14]. Indeed it has proven to stay accurate when extrapolated at relatively high heating rates.[22] This representation will not be developed furthermore, since no paper in relation with this study uses this model.

2.2.2 Heat and mass transfer model

For small particle, a uniform bulk temperature of the whole sample is used as input in the kinetic model. On the other hand, for large particles, a density and temperature fields have to be computed for each iteration which requires a heat and mass transfer model.
A large number of physical parameters such as density, thermal conductivity, heat capacity, diffusion coefficient, viscosity, emissivity, permeability are needed to describe heat and mass transfer. They are supposed to vary according to the surrounding conditions. For example, the apparent conductivity varies with the type of wood, moisture content, porosity, and orientation of the structure as well as temperature [9]. Unfortunately, there is a lack of information on their behavior in the scientific literature and sometimes simplistic approaches that better fit the experimental data are chosen [24].
Moreover, in large particle description, the two models are strongly coupled. Indeed, the temperature history inside the particle has a major impact on the kinetics but the density of the char also governs the residence time of the volatiles, the internal pressure, and the thermal properties of the porous medium. The complexity of these inter-dependencies leads to the development of many 1-dimensional models to reduce the calculation time of the simulations.

To solve the mass and heat transfer model, the energy conservation equation must be respected over the entire domain, assuming thermal equilibrium between the gas and solid phase [23]. In the case of a 1 dimensional model, it takes the simplified form of :

$$\rho C_p \frac{\partial T}{\partial t} = K_s\left(\frac{b}{r}\frac{\partial T}{\partial r} + \frac{\partial^2 T}{\partial r^2}\right) + (-q)\left(-\frac{\partial \rho}{\partial t}\right) \tag{2.2}$$

Where C_p [J/kg K] is the particle specific heat capacity, K_s [W/m K] is the spatially averaged particle thermal conductivity, r [m] is the radial position from center, b is the geometrical factor (b = 1 for cylindrical coordinate and 2 for spherical coordinate), q [J/kg] is the heat of pyrolysis that is locally produced by the reactions [43].

2.3 Large particle pyrolysis experiments

A substantial part of the pyrolysis experiments have been conducted on large particles and here are presented the most relevant data that can compare with the results of this study. The different experimental results will be interpreted in order to understand the effect of the main parameters such as the reactor temperature (or heating rate) and size of the particle on the mass loss, temperature across the samples and conversion time.
Remark : among the existing experiments, there are two different ways of heating the wood sample. The first one, characterised by a heating rate, is suitable for slow pyrolysis and consists in heating the sample and the reactor at a chosen rate from room to setpoint temperature. [9, 15, 21, 24, 41, 42] The second one, characterised by a pyrolysis temperature, is suitable for fast pyrolysis and consists of preheating the reactor to the setpoint temperature and then inserting the sample while maintaining the setpoint temperature [2, 21, 31, 36, 43, 44].

2.3.1 Devolatilization

In a TGA experiment, also called DTGA for *differential thermogravimetric analysis*, an important result that characterize the biomass devolatilization is the history of the sample mass and its time derivative, i.e. the mass loss rate [18].

Particle size influence

In a thesis published in 1997 by Miller and Bellan [16], the first multi-component kinetic model is developed to describe the pyrolysis of different particle sizes. The model is found to be incoherent for large particles, due to the fact that the coupling effects between transfer and kinetic models are not described accurately. It is compared to a previous experiment result and it is clear on figure (2.4) that the bigger the particle size, the slower the loss of mass. This is due to the internal heat transfer that is slowing down the pyrolysis inside the particle, especially at the core location.

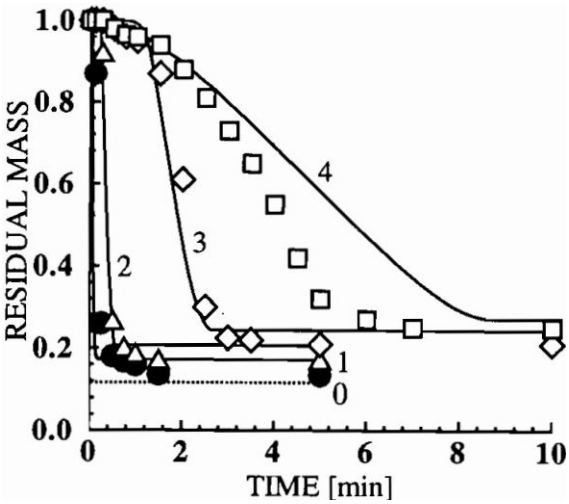

Figure 2.4: Comparison of experimental residual mass evolution for isothermal pyrolysis at 773K [26] with the full particle model in solid lines [16]. The particle diameters are 0.5mm (dots), 3mm (triangles), 8mm (diamonds) and 20mm (squares).

Heating rate influence

In 2001, an experiment is conducted by Di Blasi on large wood cylinders [15]. This is a parametric study on the heating rate while the wood particle dimensions stay constant (diameter = height = 4 [cm]). Different radiant heating values from 36 to 80 $[kW/m^2]$ are applied to the sample. It is deduced on figure (2.5) that the higher the heat flux the faster the devolatilization, since a higher heat flux generates higher temperature rising rates and faster pyrolysis.
Moreover, the experiment was carried out on different types of wood (Beech and Pine among others). Above 49 $[kW/m^2]$, the mass loss rate curve for beech wood (figure 2.5) presents a peak and then a second step of devolatilization at lower rate. The first peak comes from the carbonization of the surface subjected directly to the high external heat transfer while the second part of the devolatilization takes place via internal heat transfer at lower rate. On the other hand, on the equivalent curve for Pine wood, the peak is not as clearly visible because it has a higher content in extractives that may inhibit the reaction and a higher lignin content that has a lower reactivity [15].

At low heating rates such as 10 [K/min], it is possible to distinguish a two-peak gas production rate and thus a mass loss of the same shape (figure 2.7) which is due to the decomposition at different temperatures of hemicellulose, cellulose and lignin (figure 1.1). At high heating rates, this mass loss profile turns into a single peak because all three components of the lignocellulosic biomass are degraded simultaneously [21].

Plotting mass loss versus temperature offers an interesting perspective to better understand visually the impact of the heating rate on pyrolysis. This is done in a paper published in 2008 by Ranzi [27]. In figure (2.6) it is easy to see that with faster heating, the sample reaches a higher temperature before pyrolysis has time to start, meaning that the pyrolysis is truly occurring at higher temperature.

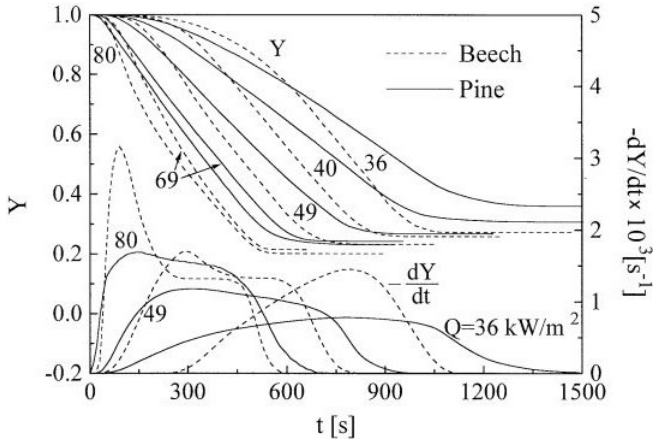

Figure 2.5: Time profiles of solid mass fractions and time derivatives of the solid mass fractions for woods exposed to several radiations intensities.

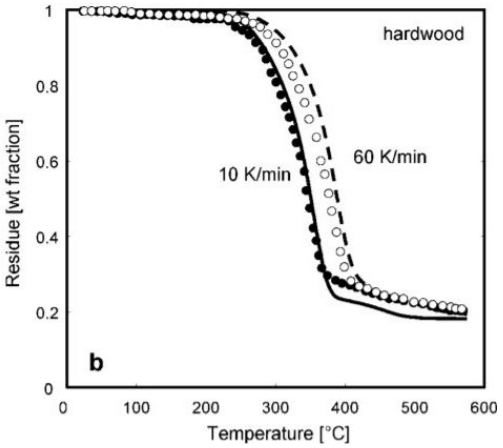

Figure 2.6: TG curves of hardwood biomass at different heating rate (points: data, lines: models)

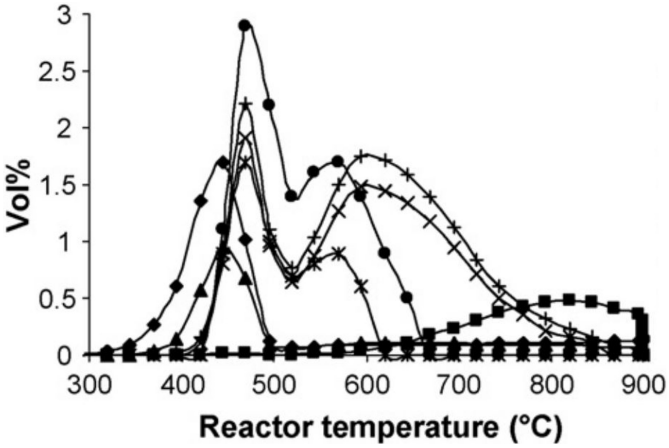

Figure 2.7: Double-maxima gas release profiles (heat rate = 10[K/min]).

2.3.2 Sample temperature

The other variable of interest in a DTGA experiment is the temperature history of the sample.

An experiment is carried out in 2013 by Gauthier [2], on a large wood cylinder where temperature is recorded at the center and near the surface. In this experiment, the preheated reactor temperature is fixed, rather than the heat flux. A comparison with an inert ceramic under the same conditions reveals that the rise of temperature at the center of the wood particle is slowed down from 200 to 450[°C] and then increased until it reaches the temperature setpoint of 800[°C] (figure (2.8)). The range from 200 to 450[°C] correspond approximately to the decomposition temperatures of cellulose, hemicellulose and

lignin and to the devolatilization period. It is widely accepted that endothermic reactions occurs during this period due to the devolatilization. At 450[°C] the devolatilization ends (not shown here) but the rise of temperature is drastically increased, due to an exothermic reaction occurring in the solid. The literature is not consistent in terms of the cause to this exothermicity . It is according to Bilbao et al.[33] due to the lignin decomposition, according to Koufopanos and Di Blasi [34, 15] due to secondary reaction between volatiles and char, according to Strezov et al. [35] due to the tar cracking and according to Park et al. [36] due to the existence of an intermediate solid between the biomass and the charcoal.

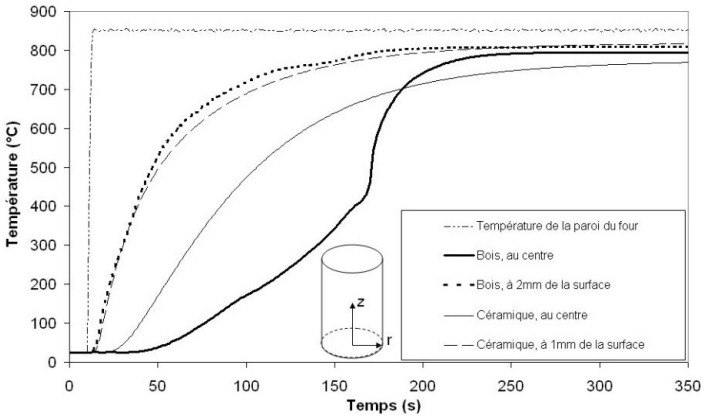

Figure 2.8: Evolution of the internal temperature in the centre and near the surface of dry wood and ceramic samples for a pyrolysis temperature of 800[°C].

A parametric study of different heating rates under the same conditions as above is also developed in 2013 by Gauthier [2] and is presented on figure (2.9). Altough the curve representations are more usual on figure (2.9), the choice to represent the temperature rise vs temperature itself on figure (2.10) gives more details and it is then easier to extract relevant information, for example changes in the endo- and exothermic behaviour of the biomass. On figure (2.10), the two inflexion points mark the beginning of two equivalent endothermic reactions and the third peak of temperature increase marks a strong exothermic reaction.

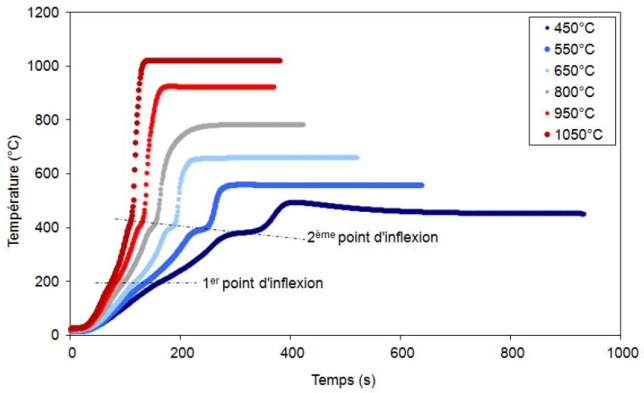

Figure 2.9: Temperature curves at the centre of a wood particle.

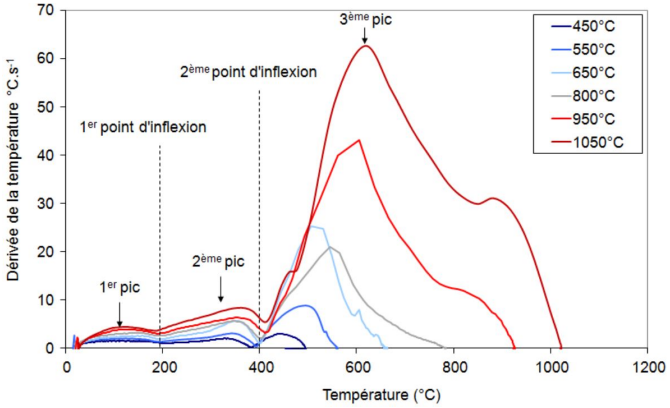

Figure 2.10: Temperature rise vs temperature at the centre of a wood particle.

2.3.3 Conversion time

The conversion time is the time it takes the biomass conversion ratio reaches to X = 0.9. The conversion ratio is defined as :

$$X = \frac{\rho_0 - \rho}{\rho_0 - \rho_e} \tag{2.3}$$

Where ρ_0 and ρ_e are respectively the initial and final particle densities. In the figure below (2.11) by Rezaei et al. [43], it is used to demonstrate that to a given pyrolysis temperature or heating rate correspond a critical particle size above which the system is limited by the internal heat transfer.

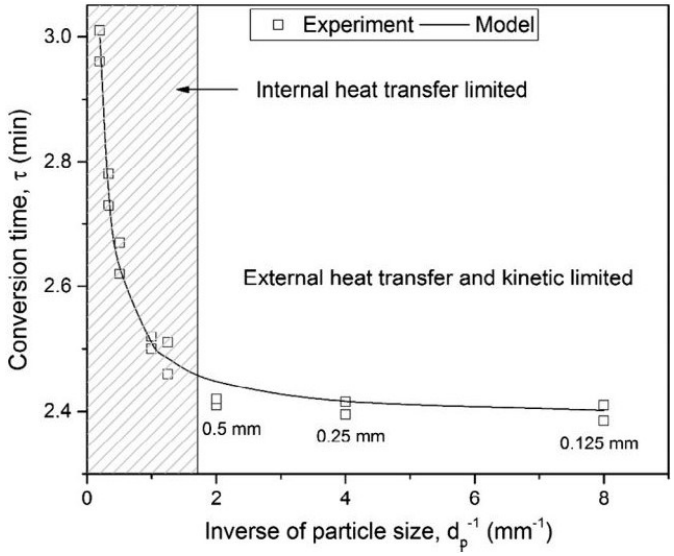

Figure 2.11: Experimental and theoretical evolution of conversion time versus inverse of particle size at the pyrolysis temperature of 500[°C] (d_p = 0.125–5 mm)

Chapter 3

Setting up of the test bench

3.1 Test bench installation

This section focuses on a chronological summary of the steps that made up the planning and implementation of the test bed from January to May 2021.

3.1.1 Equipement gathering

First, the search of specific instruments that had to be ordered to specialised companies was a priority. These instruments were a balance, a PID controller, 10 type-K thermocouples and a data logger. An old data logger from the laboratories (`PREMA3040`) was available but after testing, the compatibility with a convenient software was found out to be difficult. Another data logger from the UCLouvain Mechanical Testing, Structures and Civil Engineering laboratories (`Agilent34970A`) was chosen for the data acquisition and a user-friendly software (`ContactProIV`) was properly installed with the help of Antoine Bietlot on a portable computer that belongs to the UCLouvain. A PID was hopefully available and ready to use in the laboratories of the UCLouvain. Then, with the advices of Hervé Jeanmart, Frank Hesbois and Alex Bertholet, a balance was ordered to the Sartorius company. Finally, Frank Hesbois ordered the 10 thermocouples to the Thermibel company.

3.1.2 Plans & adaptation to reality

Second, the plans of the reactor from last year were refined with Arnaud Lion and approved by Pr. Hervé Jeanmart. Then, the technicians started the reactor assembly with additionnal supervision and oral instructions to ensure a good consistency with the objectives of the experiment. Some adaptations had to be made in relation to the conditions of the laboratory, the equipment available and the complexity of the operations for the technicians. For instance, the cover flange was twice as thick as compared to the plans because it did not change the conditions of the experiment. At that moment, it was the only flange available and an extrusion of half its thickness was a tedious work. However, it had the disadvantage of making a heavy cover for the reactor and a workshop crane was now necessary to lift it. Also a static scale support above a moving cover was not feasible, considering the sample reloading manipulation. The scale support had to be based on the reactor cover so that it could be lifted with the cover during manipulation (see fig. 3.8).

3.1.3 Test bench spot

Third, a place for the test bench had to be found in the laboratories. There were several requirements to make the place appropriate : an easy access with the crane, a gas evacuation, a spot for the nitrogen tank

nearby and electricity. The electricity and spot for gas tank were easy conditions to fulfill. A natural evacuation to the atmosphere was preferable to a ventilation because an aspiration could have caused air in the reactor and then, unwanted internal combustion. The evacuation was via a hole drilled through a metal wall in the laboratory. This metal mall was situated at the back of the labs and the spot for the test bench was right next to it. In order to access easily the top of the reactor with the workshop crane, it was decided that the reactor would be on a table with wheels.

3.1.4 Final preparations and overview of the bench

Fourth, with the help of the updated P&ID, Frank Hesbois installed the plastic tubes from the tank to the reactor, the copper pipes from the tank to the atmosphere, the power controller and the electrical connections of the heating ceramic. Then, the measurement equipment (balance, thermocouples and data logger) as well as the nitrogen and electrical network, were tested independently to check their correct functioning before starting the experiment.

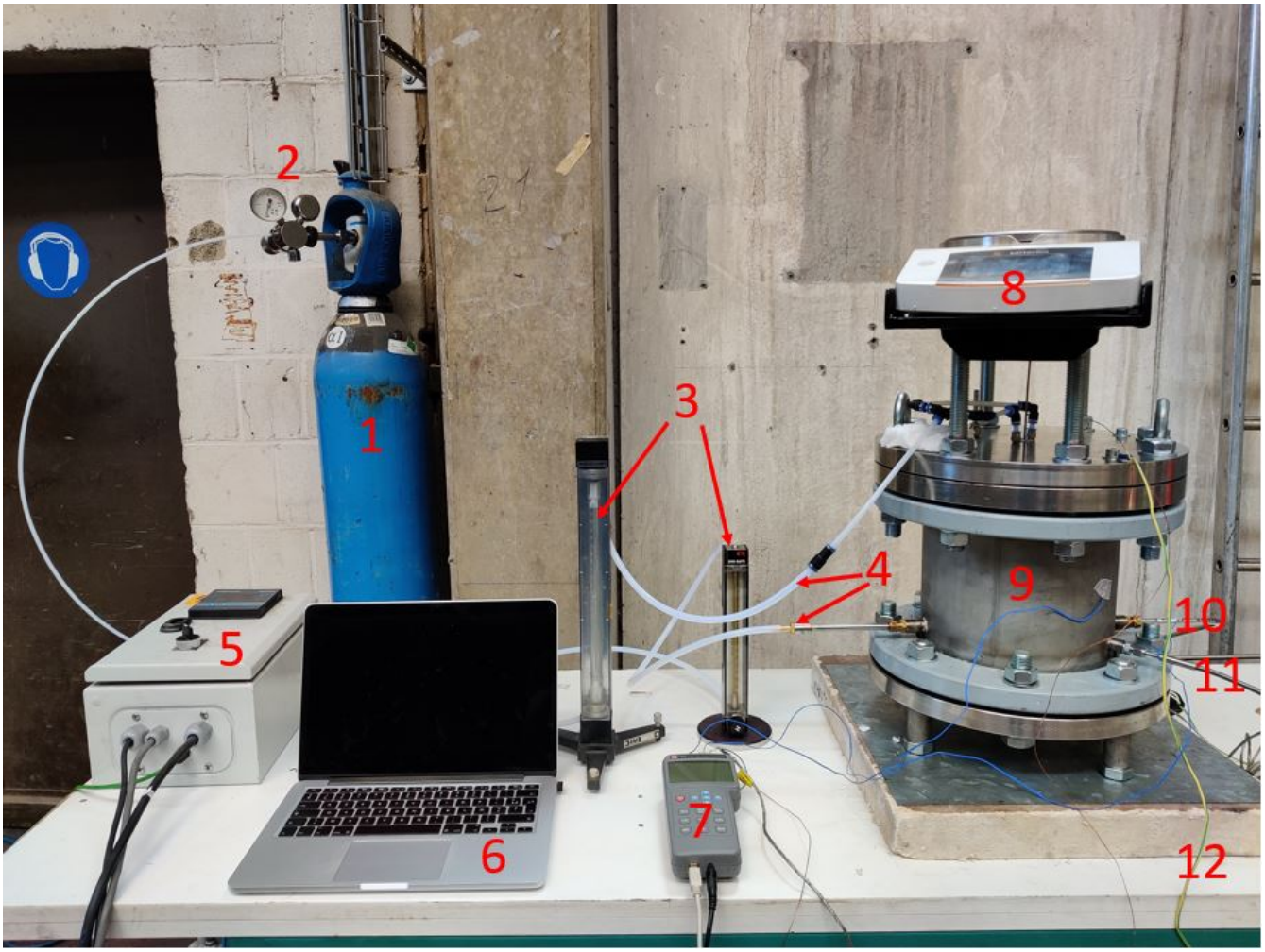

Figure 3.1: Overall picture of the test bench

Legend :

1. Nitrogen tank
2. Gas pressure regulator
3. Rotameters
4. Nitrogen inlet
5. PID temperature controller
6. Laboratory analysis PC
7. Thermocouples DAQ
8. Precision balance
9. Casing of the reactor
10. Exhaust gases outlet
11. Temperature probe
12. Electrical ground

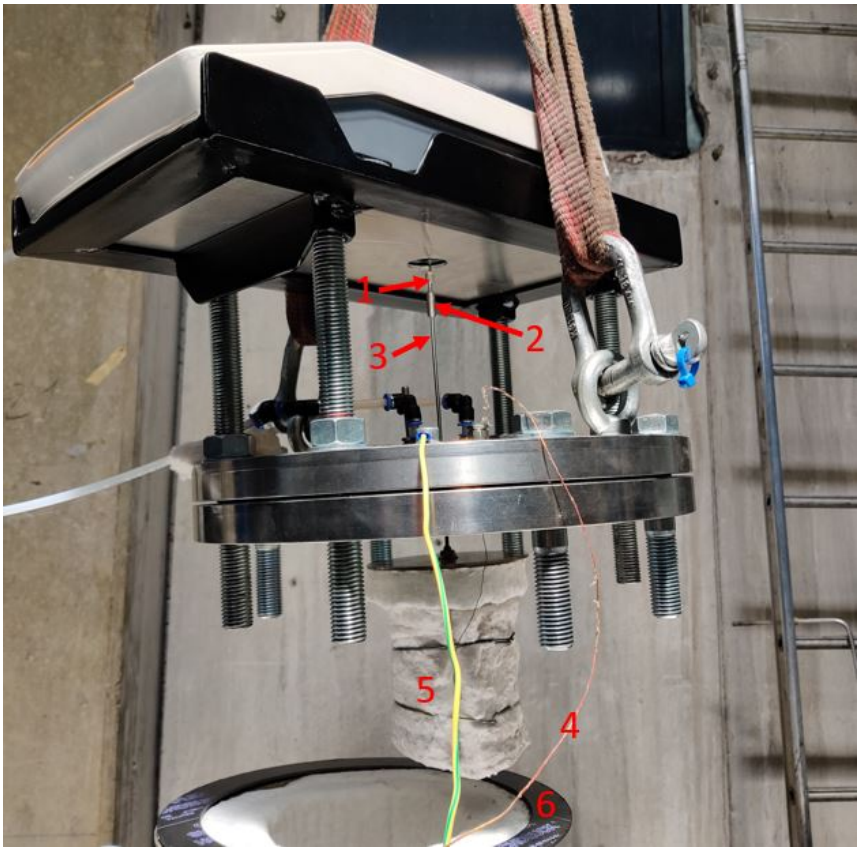

Figure 3.2: Picture of the hanging sample

Legend :

1. Weighing cable (upper part)
2. Connecting nut
3. Weighing cable (lower part)
4. Thermocouple
5. Sample isolating layer
6. Joint

3.2 Design of the reactor

In this section, the general design of the test bench will be quickly presented, as it already have been developed last year by the previous team working on it [1]. As a second step, a particular focus will be placed on the new features and changes that were brought in this year.

3.2.1 Last year design

Last year version is represented on figure (3.3). Small changes are brought in in order to refine and make the reactor more convenient to use (figure 3.4) and the new plans can be found in appendix A. Yet, the main dimensions of the sample, heating source and insulation layers remain unchanged to conserve the 1-dimensionality hypothesis of the heating.
A threaded cable is hanging from a balance and at its lower end as screw is inserted in a vertical wood cylinder. The wood cylinder is fitted in a stainless steel tube and wrapped with a layer of insulating ceramic wool that is maintained with a pressure plate on the top and a metallic thread on the side. This set of parts is called the hanging basket. One centimeter below, the ceramic slab heats 1-dimensionally the bottom of the wood sample by radiation. To maintain an inert atmosphere in the reactor, an airtight metal casing is installed around the basket and the ceramic slab. A purge gas (nitrogen) is flushing the pyrolysis volatile products in a main flow from the top of the reactor and a secondary flow from one side of the ceramic slab, i.e. the bottom left of figure 3.3. The exhaust gases are leaving the reactor by an exit tube on the bottom right of figure 3.3. Finally, a second insulation layer is set up against the inner wall of the container to reduce conduction through the walls.

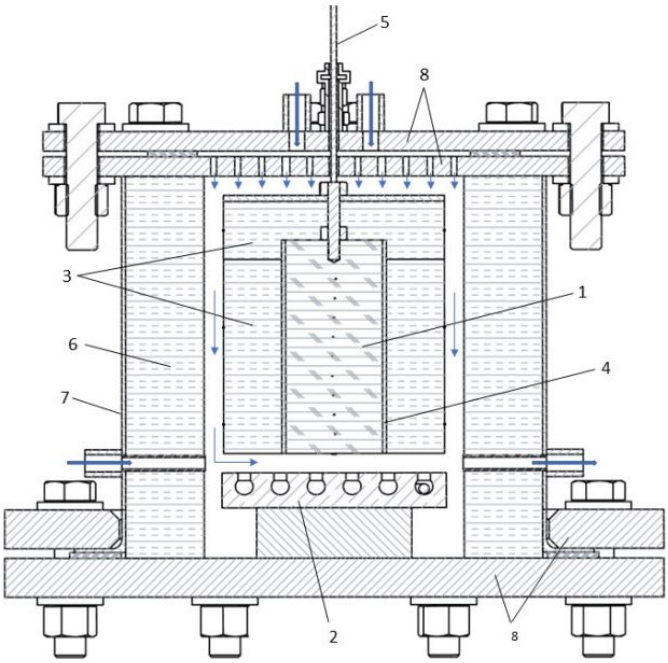

Figure 3.3: Old reactor cross-section. 1: Sample; 2: Heating source; 3: Sample insulation; 4: Insulation fixing tube; 5: Hanging cable connecting to balance; 6: External insulation; 7: Casing; 8: Clamp.

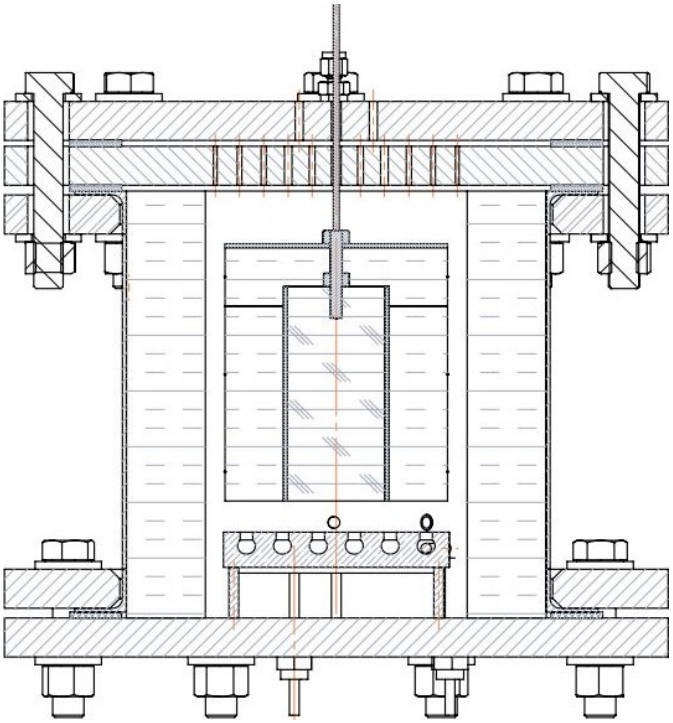

Figure 3.4: New reactor cross-section.

3.2.2 Main changes

Cover of the reactor

The main change is the new design of the cover of the reactor that allows to open it from the top and insert more easily the basket with the sample. As represented (figure 3.4), the welded joint between the cover and the outer wall is replaced with a clamp closure. The sealing of the lid is done manually using 8 bolts that tighten the cover and a clamping ring around the top of the reactor. This requires a new clamp ring and increase the reactor overall weight.

Base of the ceramic

The second change is to modify the base that supports the heating ceramic slab. In order to minimize the heat conduction to the base of the reactor and its surrounding elements, as much volume as possible is removed from the ceramic slab base. It takes the form of a flat ring supported by 4 legs (figure 3.5). The decision of the material is yet to be made and stainless steel is chosen for its strength and hardness so that even more material could be removed without threatening the solidity of the structure. The main advantages of this new design are a lower thermal inertia of the reactor and a convection phenomenon on the bottom of the slab that helps for the homogenization of its heating. An extra layer of insulating wool is also added below this new support on the bottom of the reactor.

Metal grid

The third change is the addition of a metal grid underneath the wood sample to prevent char particles from falling onto the hot ceramic, or even whole pieces of the sample in case of splitting. The grid is thin but nevertheless permeable to the passage of pyrolysis gases and is held to the stainless steel tube by a metal clamping ring located under the insulation 1 cm above the bottom of the sample (figure 3.6).

Figure 3.5: Metal base of the heating ceramic

Figure 3.6: Metal grid of the basket bottom

Sealing of the weighing cable

Moreover, the gas outlet is a long tube that goes to the atmosphere and a small pressure in necessary to drive the exhaust gases. This is why a screw cap has been fitted around the weighing cable at the point of insertion into the cover, in order to prevent backflow from happening due to the small atmospheric overpressure. To ensure that there is no interaction with the mass measurement, lubrication grease is added between the metallic parts even tough the vertical displacement of the cable is very small during the weighing.

Figure 3.7: Cable sealing

Figure 3.8: Scale holder

Scale holder

A support for the balance needs to be built and takes the shape of a metal table (figure 3.8). It is composed of four feet with screw threads anchored in the reactor lid with bolts and a metal frame that supports a metal plate. The balance is placed on the plate where a hole is pierced to let the weighing cable trough. Thus, when the sample is replaced, the balance and its holder are lifted with the lid for the duration of the operation.

3.3 Piping and instrumentation

In this study, the priority of measurements was given to a thermogravimetric analysis, which consists of measuring the variation in mass of a sample as a function of time, for a given temperature or temperature profile. These quantities, as well as the nitrogen mass flow must therefore be measured and controlled with the appropriate equipment.

3.3.1 Mass measurement

The mass measurement of the basket, performed at a frequency of 1 [Hz] by a balance with a precision of 10 mg was envisaged. A lower mass resolution could reduce the accuracy of the observations while a higher mass resolution would be useless due to the ambient noise and vibrations that were experimentally observed in the laboratory. The total weight of the basket is estimated to be around 650g, therefore the Sartorius® PRACTUM1102-1S precision balance is chosen for its 10 [mg] precision and its maximum capacity of 1100 [g]. The last requirement is a weighing hook at the bottom of the scale and it is also fulfilled by the balance.

3.3.2 Temperature measurement and control

The temperature measurement in the center line of the sample is achieved by the means of 10 type K thermocouples inserted trough the wool and stainless steel. A data acquisition system (DAQ) sample at a frequency of 1 [Hz] the signals from the 10 thermocouples and send them to a computer from the Uclouvain, which is part of the test bench. On this computer, the digital data is extracted with the help

of `ContactProIV`, a software coded in `Labview` and developed at the Uclouvain.
A PID controller monitors the temperature to reach the desired setpoint. It is linked to a thermocouple through a fast loop, and this special thermocouple is called the temperature probe. This is the only regulating thermocouple of the bench, even tough an operator always watch the temperature of all thermocouples and can stop the experiments in case of overheating. The temperature probe is placed just above a coil of the heating ceramic and should measure a temperature as close as possible to that of the resistive wire.

3.3.3 Nitrogen mass flow measurement and control

The nitrogen comes from a gas tank, flows into the reactor, mix with the pyrolysis volatile products and exits to the atmosphere trough pipes. Its mass flow rate is set to 8 [NL/min] and divided in a main stream of 6 [NL/min] and a secondary stream of 2 [NL/min]. The secondary flow is here to ensure convection at the bottom of the reactor so that the temperature is uniform and that the tars are flushed out before condensing. A too high nitrogen flow rate would cool down the pyrolysing zone while a too low flow rate would cause a hot backflow to the upper part of the reactor, an increase in the concentration of volatiles in the reactor and an uneven heating of the ceramic. As the nitrogen flow rate is subject to empirical adjustment, strict control of the flow rate is not necessary and the use of rotameters is sufficient. When the gas pressure regulator and the security valve are open, both flow rate are measured and controlled in parallel by 2 rotameters.

3.3.4 Piping and instrumentation diagram

The P&I diagram (figure 3.9) shows the general layout of the measurement, piping and control tools of the test bench. A detailed version of this layout with a precise legend of the attributes is available at appendix B. One can note that the mass flow controllers here are replaced with rotameters for economical reasons.

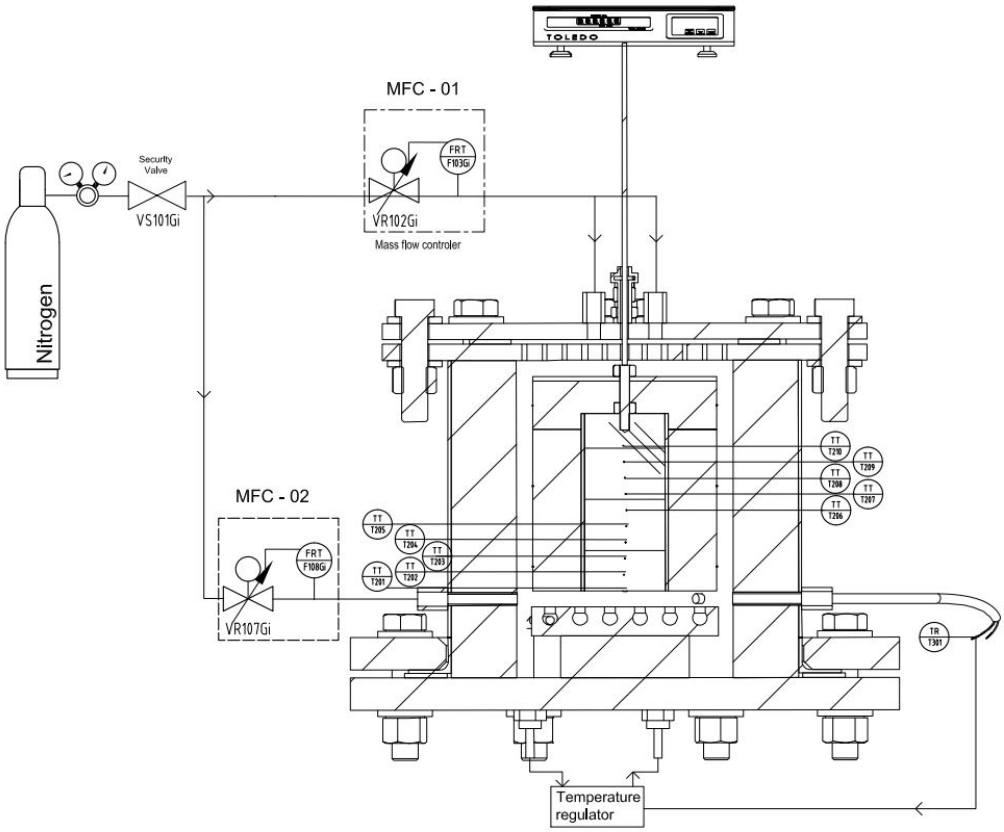

Figure 3.9: Piping and instrumentation diagram

3.4 Experimental procedure and risks

Each experience has a procedure that should be as much respected as possible in order for the experience to succeed, i.e. to have proper results and guarantee the safety of the operator. This is the content of this section.

3.4.1 Risks

In the present experiment, a heating source, heavy elements, electricity and chemical reactions are inevitably sources of dangers. The main risks and the solutions brought in to reduce them at an acceptable level are presented in the next paragraphs. A detailed risks analysis had to be written during this year and is accessible in appendix [C].

Dangers

- Gas intoxication : Some gas products of pyrolysis are very toxic to breathe, like carbon monoxide.
- Burns : After one hour of heating the device, a lot of external parts are at temperatures higher than 40[°C] and could cause burns.
- Fire : In case of uncontrolled overheating, a fire could start and spread in the laboratory. The outlet gases can ignite if the temperature is sufficiently high and also cause fire.
- Mechanical injury : There are heavy moving parts and parts at height that could fall on a person.

- Electrocution : While heating, hot parts could deteriorate or move and cause conduction to the metallic structure of the reactor that would rise up to 220 [V], charging as a huge capacitor. The effect of touching it while standing on the ground could cause serious injury.

Solutions

- Wearing personal protective equipment (PPE).
- Outer thermal insulation on reactor wall and outlet pipe.
- Copper duct cooling the outlet gas before ejection into the air.
- Layer of thermal insulation between the reactor and the table.
- Use of a CO concentration analyzer.
- Earthing of the test bench.

3.4.2 Procedure

Secondly, a sample is consumed for each experiment and thus needs to be replaced between each cycle. This generate a lot of mechanical manipulations for the operator. A detailed user manual had to be written during this year and the original and complete version is accessible in the appendix [C]. However, the main steps of this handling are presented below :

1. Opening the reactor lid and lifting it with the workshop crane. (see photo : 3.2)
2. While the lid is hanging, removing the thermocouples from the sample, the basket from the lid and the sample from the basket.
3. Reloading the sample by following the inverse three operations.
4. Closing and sealing the reactor.
5. Turning on the nitrogen flow rate to purge the reactor.
6. Reducing the nitrogen flow rate and turn on the heating ceramic.
7. When mass loss is not occurring anymore, turn off the heating ceramic.

Chapter 4

Experimental part

4.1 Conduct of the experiments

Five experiments that produced a complete pyrolysis were conducted. All of them were stopped because of an electrical problem linked to the overheating of the ceramic slab. Here are the descriptions of the observations during and after these experiments and an explanation for each phenomenon that occurred.

4.1.1 General behavior

During all the experiments, leaks were happening. Indeed, the reactor complete sealing is only possible during the experiment because this is the moment where the fumes are getting out of the casing and fumes leaks are the best tool to know where to tighten the bolts.
The main leaks happen between the moving pieces of the metal casing. It is situated at the electrical cable glands, at the clamp ring, at the thermocouples entry and at the weighing cable. The electrical cable are systematically removed between each experience to check the state of the ceramic slab and this is why leaks are often occurring at the cable glands. Another leak between the cable glands and the reactor is also sealed with glue. Almost all the leaks could be resolved by tightening the bolts or the cable glands or with aluminium adhesive paper and insulating wool. However, the insertion of the weighing cable into the cover of the reactor could not be sealed because any contact with the cable would have caused an interaction with the mass measured by the scale. The best solution is to reduce the hole with the help of an inner ring screwed on the cable (3.7) and almost in contact with the lid of the reactor. Solid grease is added in the remaining holes but is not strong enough to contain the pressure at the peak of pyrolysis and always slips out.

4.1.2 Experiment 1 :

Conditions

- Nitrogen flow rates are at their nominal values (6 and 2 [NL/min]).
- Temperature probe is 5 [mm] above the ceramic.
- No metal grid below the sample.
- Distance from ceramic slab to surrounding insulation had not been checked.

Observations

During the experiment, the probe reaches 560[°C] then momentary short circuit (current exceeds 16 [A]) which blow the safety circuit breaker. Reconnecting the power supply allows the temperature to rise by 20[°C] before a new short circuit, then 10[°C], 5[°C], etc. After the experiment, there is some thermo-chemical reaction with the ceramic at the resistance connections and breaches in the wire near the connections.

Explanations

It is likely that the short-circuit happens between one terminal and the ground that was set on the metallic armature of the reactor. As the temperature probe is not close enough to the resistive wire, the temperature in the ceramic exceeds the setpoint. This overheating causes thermo-chemical reactions with the ceramic at the hottest points (i.e. the first and last grooves that are closer to insulation). This phenomenon degrades the solid structure until the metallic connections would be close enough to the stainless steel support of the ceramic to produce a short-circuit.

4.1.3 Experiment 2 :

Conditions

- Same conditions as experiment 1.
- Connection to the resistance is now shorter (broken end turns).
- Packing of the insulation around the ceramic so that nothing touches the resistance.

Observations

During the experiment, the probe reaches 650[°C] then momentary short circuit (current exceeds 16 [A]) which blow the safety circuit breaker. Reconnecting the power supply allows the temperature to rise by 20[°C] before a new short circuit, then 10[°C], 5[°C], etc. After the experiment, there are more thermo-chemical reaction with the ceramic at the resistance connections and more breaches in the wire.

Explanations

Same phenomenon as in first experience (4.1.2), so only packing the insulation around the ceramic does not solve the overheating problem and the root of the problem is linked to the temperature probe.

4.1.4 Experiment 3 :

Conditions

- New ceramic slab.
- Nitrogen flow rates are at their nominal values (6 and 2 [NL/min]), then secondary flow is cut off at 28 [min].
- Temperature probe is in direct contact with the ceramic.
- A metal grid is present below the sample.

Observations

The grid reaches 550[°C] and then loses its heating rate and rises slowly to 630[°C]. At 28 minutes, secondary flow is switched off and the ceramic temperature rises sharply to the setpoint at 750[°C]. The grid follows slowly and rises to 660[°C]. At 52 minutes, error indicated on the PID, loss of temperature, and the power is switched off. After the experiment, the temperature probe is molten on the ceramic and causes an open circuit in the middle of the resistance.

Explanations

With the rising temperature, the probe becomes soft and goes down close enough to the resistive wire to create an electrical arc. The probe then melts away and causes an open circuit and the loss of power causes the temperature to go down (figure 4.1). Besides that, there are no reactions on the connection of the ceramic while it kept the setpoint temperature for 15 [min], so cutting the secondary flow is not a problem for hot spots and helps for faster heat rate. Finally, the added grid already eliminates potential problems with char particles.

Figure 4.1: Melting of the probe on the ceramic

Figure 4.2: Protecting ceramic tube above the wire

4.1.5 Experiment 4 :

Conditions

- Nitrogen flow rates are almost cut (0.5 and 0 [NL/min]).
- Temperature probe is in light contact with the ceramic and protected by a ceramic tube (figure 4.2).
- A metal grid is present below the sample.
- The insulation is packed around the ceramic so that nothing touches the resistance but the ceramic is off-centre of the insulation hole and one connection is closer to the insulation than the other.

Observations

At 20 minutes, the ceramic reaches the setpoint of 650[°C] and starts to oscillate with an amplitude of 30[°C] and a period of approximately 90 [s]. At 54 minutes, the temperature starts to go down and 10 minutes later, the power is switched off. After the experiment, there is a thermo-chemical reaction with the ceramic and an open circuit at the resistance connection that is closer to the insulation.

Explanations

The temperature probe is close to the real temperature of the wire but in absence of convection due to the cutting of the primary and secondary nitrogen flow, the heating of the ceramic is strongly heterogeneous and the heat accumulates at the connection that is closer to the insulation. At some point, the temperature is too high for the ceramic structure to keep its stability, creating an open circuit and a loss in temperature. It was then a complete error to cut the primary and reduce the secondary flow to a quarter of its nominal value.

4.1.6 Experiment 5 :

Conditions

- Nitrogen flow rates are lower than nominal values (3 and 0.5 [NL/min]).
- Connection to the resistance is now shorter (broken end turns)
- Temperature probe is 1 [mm] above a heating groove and protected by a ceramic tube.
- A metal grid is present below the sample.
- A layer of the bottom insulation is removed to ensure a good convection below the ceramic.

Observations

At 15 minutes, the ceramic reaches the setpoint of 650[°C] and starts to oscillate with an amplitude of 3[°C] and a period of approximately 40 [s]. At 54 minutes, a short-circuit blow the safety circuit breaker and thus the power is switched off. After the experiment, there is a thermo-chemical reaction with the ceramic and an open circuit, as illustrated on figure (4.3).

Explanations

It is likely that the short-circuit happens between one terminal and the ground that was set on the metallic armature of the reactor. It is caused by the degradation the solid structure until the metallic connections are be close enough to the stainless-steel support of the ceramic to produce a short-circuit. The initial overheating is due to the fact that the wire is running with 15% more current than the rated current.

Figure 4.3: Molten ceramic

4.1.7 Discussion

The heat source environment is currently not robust to overheating. Nevertheless, with a series of minor changes, the main design of the experiment could be kept, in order to run it successfully. These changes are discussed in section 5.1.1.

4.2 Result of the experiments

Out of the 5 thermal pyrolysis cycles performed in this study, both experience 1 and 2 are calibrating tests while experience 3,4,5 are performed for data collection. Therefore, these three last experiences will be called cycle 1,2,3 respectively and their results will be discussed and compared to the previous literature to assess their validity.

4.2.1 Reproducibility

Cycles 1 and 2 are similar in terms of heating rate and heating period and the devolatilization curves overlap up to 50 min (see figure 4.4). Nevertheless, the average setpoint reached by cycle 1 is 50[°C] higher than that of cycle 2, which leads to two divergences between the curves of the experiments. Firstly, the sample medium of cycle 1 dries faster than that of cycle 2 and rises faster in temperature. Secondly, from 50 min onwards, the devolatilization of cycle 1 becomes more intense and seems to be complete due to the sudden stop of pyrolysis at 65 min, unlike the second one.
The heating behaviour of cycle 2 and cycle 3 is not the same either (see figure 4.5). Cycle 3 heats up faster than cycle 2 because the heating wire is reconnected shorter, the resistance drops and the power increases by about 15%. In addition, once the setpoint is reached, the temperature at the grid in cycle 3 oscillates much less than in cycle 2. This is due to the position of the regulating probe, which was previously installed above a ceramic groove and is now installed above an electrical winding groove (see figure 4.2) where the air heats up much faster due to a change in radiation.
In conclusion, the disparity of heating conditions is a major threat to the reproducibility of the experiment and a unique heating set up must be established.

4.2.2 Thermal inertia

On figure 4.4 the full heating cycles 1 and 2 are presented, i.e. the experiment that is performed with only 2 thermocouples, and the most relevant experiment among those performed with 6 thermocouples. Due to an open circuit in the heat source, these cycles experienced a loss of heat at 52 and 54 minutes respectively and yet, pyrolysis continues for up to 65 minutes in both cases.
This is partly due to the thermal inertia of the wood particle. In fact, the internal heat transfer of the particle causes a time shift between the temperature at the grid and the temperature at the centre (i.e. z = 5.5 [cm]), and this is well illustrated (figure 4.4 and 4.5). When the grid cools down, the temperature remains high in the centre of the wood sample and a self-sustaining devolatilization keeps on happening.

4.2.3 Mass loss rate

In addition to this, devolatilization peaks at around 60 [min] (figure 4.6), the peak seems too high to be due to thermal inertia alone and the curve does not resemble anything that is expected from models developed in the same geometry as done by Mottiat and Benoit [1] and by Gronli [9]. There is therefore another effect that causes the general temperature increase observed in figure 4.5 between 50 and 60 minutes and this effect is either shrinking, splitting or reaction exothermicity. Shrinking enhance convection heat

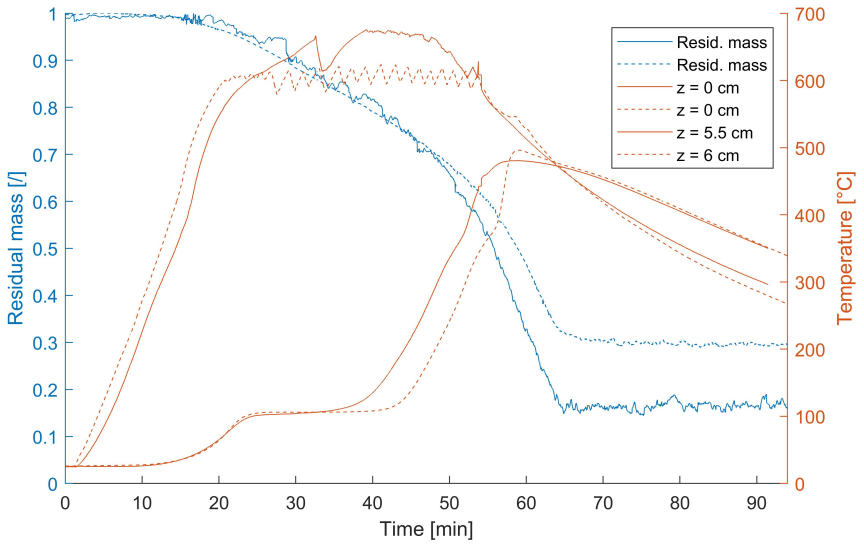

Figure 4.4: Mass and temperature vs time in the wood cylinder (solid = cycle 1, dashed = cycle 2)

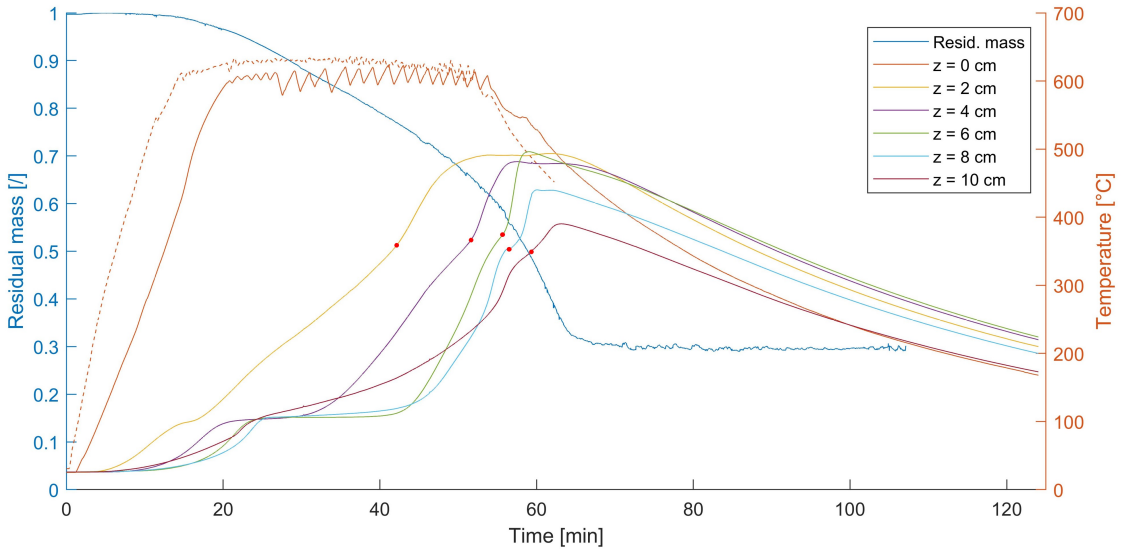

Figure 4.5: Cycle 2 : Mass and temperature vs time in the wood cylinder (dashed lines = grid cycle 3)

transfer gradually but would not produce such sharp temperature inflexion points on figure (4.5) (red dots). It could be the result of an exothermic reaction occurring at certain temperature in these precise heating conditions because the inflexion points are not much spaced in temperature. But it is more likely to come from at least a mix of exothermic reactions and an abrupt increase in convection and radiation caused by the splitting of the sample that is systematically observed at the end of each experiment (see figure 4.9,4.11). The red dots would then mark the progression of the crack throughout the height and along the fibers of the wood cylinder. Unfortunately, in view of the poor control of the heat source and the resulting quality of the data from the experiment, no definitive conclusions can be drawn at this point.

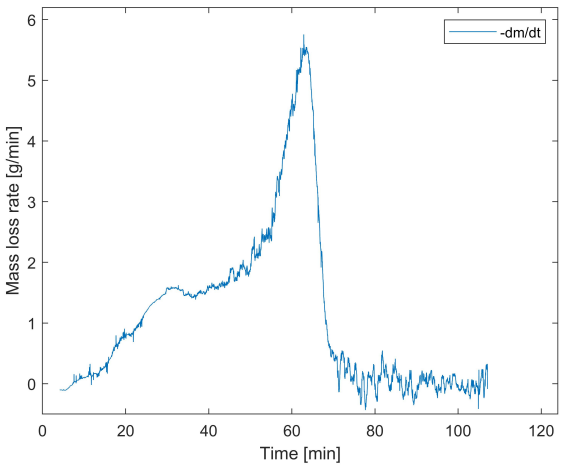

Figure 4.6: Cycle 3 : Mass loss rate vs time in the wood cylinder

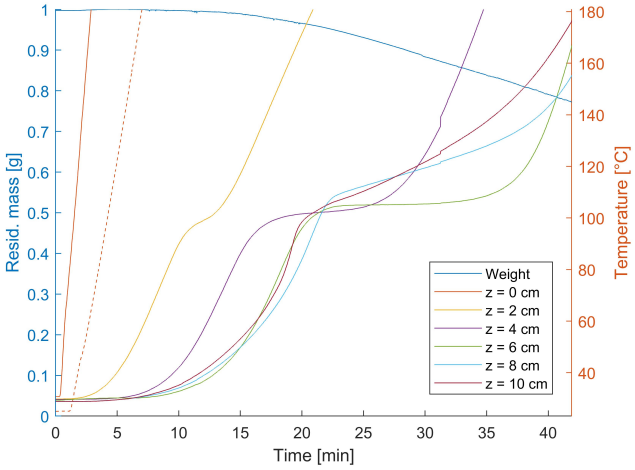

Figure 4.7: Cycle 3 : Mass and temperature vs time in the wood cylinder

4.2.4 Drying and 1-Dimensionnality

Inside the particle, there is a temperature plateau whose duration increases the closer one gets to the centre of the wooden cylinder (see figure 4.7). This is caused by the evaporation of the remaining moisture in the wood at around 100[°C]. Unfortunately, before and during drying, the temperature for z = 8 and z = 10 [cm] rises faster than at the centre, which implies a relatively high conduction into the stainless steel tube surrounding the sample, questioning the one-dimensionality of the experiment. Nonetheless, after drying, the temperatures return to a decreasing function of z. This is due both to the transient nature of the heating in the sample and shrinking and splitting that occurs after the drying process, enhancing convection and radiation through the wood in the vertical direction.

4.2.5 Residual solid : shrinking, cracking and swelling

On leaving the reactor, the biomass has obviously changed its chemical composition as the remaining solid is mainly composed of char.
However, the shape and structure of the particle has also changed and the most visible effect is the shrinkage of the solid matrix. Here, a relative radial shrinkage of 38% and axial shrinkage of 14% is observed. The radial shrinkage is in good agreement with the scientific data [2], but the axial shrinkage is lower than the usual values around 25%.
Another effect observed is the cracks at the base of the char sample where the rings of the trunk can be seen. Most of the cracks are small, parallel and directed towards the centre of the tree rings, but larger cracks directed in random directions are also present (see figure 4.11). These larger cracks run up the length of the sample along the fibers of the wood, so the sample is said to have split (see figure 4.9). These cracks are probably due to the mechanical stresses that arise from heterogeneous shrinking and decreasing density of the medium. A surprising effect is the swelling of the char structure at its base, which may be part of the reason for the cracks. Finally, char powder collected by the metal grid is systematically observed at the end of the disintegration of the wood particle, due to the weakening of the structure.

Figure 4.8: Radial and axial shrinking

Figure 4.9: Sample splitting side view

Figure 4.10: Char dust

Figure 4.11: Sample splitting bottom view

Chapter 5

Improvements and future works

5.1 Improvements

During the heat cycles, the design of the reactor is tested and then appropriate modifications can be considered to improve some of its specific performances. The reproducibility, safety and one-dimensionality of the experiment can be improved through changes to the heat source, reactor sealing and sample basket respectively.

5.1.1 Heat source

The heat source overheating and destruction is the major problem of the design of the test bench. Since the heat source must be repaired between each experiment, no similar heating condition can be reproduced over and over, so no comparison between experiences is really meaningful at this stage which makes it impossible to envisage a more detailed study.

Resistive wire overeating

Firstly, in order to avoid wire melting, an open circuit and unwanted reactions with the ceramic, the wire must be prevented from overheating. This can be accomplished simply by procuring a resistor with an integrated temperature controller that has industrial precision and has been extensively tested, as opposed to laboratory set-ups.

Conduction through the base

Secondly, to prevent short circuits that stop the heating cycle and melt the ceramic and the wire, the conduction paths through the metal base of the ceramic to the metal structure of the reactor must be cut. The simplest solution is to add a layer of high-temperature resistant insulation between the ceramic and its base.

Particle deposits on the wire

Thirdly, in order to avoid unpredictable effects, the fall of bodies (char particle, piece of insulation) by gravity on the exposed wire must be minimised. A metal grid has already been installed to deal with char particles, and a careful check of the insulation before each pyrolysis cycle should be sufficient to ensure that no pieces will fall off during the experiment. Indeed, such deposits on the ceramic are very rarely observed at the end of the experiments.

Hot spots near walls

Fourthly, in order to avoid the degradation of components at high temperature, hot spots near the insulation walls should be removed. For this purpose, the width of the ceramic, which is unnecessarily large for the one-dimensionality of the experiment, can be reduced. In addition, a check of the gas layer between the heating ceramic and the insulation can be performed at the beginning of each experiment to ensure that the insulation walls have not moved.

Heterogeneous temperature

Fifthly, for the same reason as above, the temperature of the ceramic should be homogenised as far as possible. This is because the density of the wire is unevenly distributed over the ceramic and the heating is heterogeneous. This effect can be mitigated by inducing convection on the surface of the ceramic with the help of the secondary nitrogen flow. For a constant heat flow to the wood sample, it is better to use a higher power at the ceramic combined with a higher convective nitrogen flow.

5.1.2 Reactor sealing

In order to conduct experiments safely, there should be no leakage of pyrolysis gases that could cause short or long term poisoning of the test bench operator. Therefore, the remaining leak at the insertion of the weighing cable into the reactor must be sealed. In addition, this leak causes hot gases to rise to the top of the sample and affects the one-dimensionality of the experiment.
It is not possible to seal the weighing cable and create a static pressure because it would interact with the mass loss measurements. Therefore a dynamic pressure should be created by means of a pipe bringing nitrogen at high speed vertically towards the entrance of the annular hole (see figure 5.1) delimited on the one hand by the cable and on the other hand by the hole in the reactor shell. Park et al. stated that the internal pressure generated inside a large particle could reach up to 1.4 [atm] during a fast pyrolysis at 800 [°C]. In this experiment, considering the slower heating rate and the pressure drop through the porous sample, a dynamic overpressure of 0.2 [atm] should be envisaged in the first instance to counter the pressure of devolatilization.

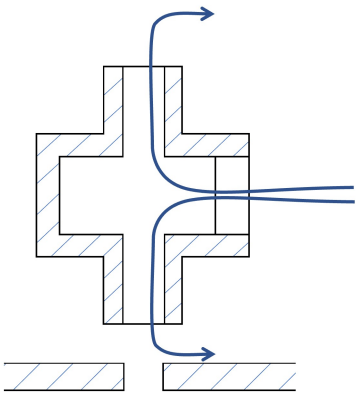

Figure 5.1: Nitrogen flowing through a metal piece along the weighing cable (not represented)

5.1.3 Sample basket

In order to ensure the one-dimensionality of the experiment, the conduction to the top of the sample through the stainless steel tube observed on figure 4.7 must be reduced. For this purpose, the thickness of the tube can be reduced as well as its length so that the wood sample is allowed to extend slightly beyond it. The wood sample is still surrounded by insulating wool. Thus, the stainless steel tube base is no longer subjected to direct radiation or convection.

5.2 Future works

Once all the technical problems of the test bed have been overcome by the improvements made, it is possible to consider the future experiments that are most relevant, i.e. those that are possible with the test bench and for which the results are not yet well established in the scientific literature.

5.2.1 Wood pre-drying

Firstly, the wood samples should be pre-dried at 115[°C] during 3 hours as done by Park et al. , as the drying phenomenon influences the pyrolysis, makes the models more complex and is not the object of interest. At least 3 experiments should be performed under the same conditions in order to validate the reproducibility. Once the reproducibility is validated, the mass and temperature measurements can be performed independently, to avoid mass interaction due to the thermocouples.

5.2.2 Model comparison

Once reliable results are obtained, a comparison with a model makes a lot of sense. To be consistent with last year's work, the Miller and Bellan model used in the SPY algorithm developed by Jeanmart and Blondeau at UCLouvain should be used. Compare the results of the model with those of the experiment in order to draw conclusions about the unidimensionality as well as about the phenomenon itself.

5.2.3 Temperature parametric study

This year, temperatures only reached a maximum temperature of 650[°C] in the woods. Nevertheless, the experiment is designed to reach 800[°C]. A parametric study of the pyrolysis as a function of the temperature set point and the heating power can be conducted. Its impact on devolatilization, residual mass and heat penetration in the particle would be compared with the numerous examples in the scientific literature.

5.2.4 Anisotropy characterizing

The anisotropy of the biomass sample can be studied very easily by orienting the wood fibres horizontally rather than vertically. A significant change in the conduction, devolatilization and cracking of the wood can be expected and would be interesting to verify.

5.2.5 Biomass type

In a later stage another type of biomass such as a phenolic impregnated carbon ablator (PICA) could be used in the reactor. Indeed, this material is typical of the experiments of another part of the scientific community that is making similar research efforts on pyrolysis in the field of aerospace application. An analysis of the previous results and those obtained with PICA could be a first step to allow a better comparison between the two separate pools of results

5.2.6 Gas analysis

Finally, in order to exploit the full potential of the test bed, an analysis of the outlet gases could be envisaged but would be a major undertaking and would require efforts to redesign the reactor and the gas outlet.

Conclusion

The aim of this experiment was to study the one-dimensional pyrolytic behaviour of a wood sample in an inert atmosphere, first with beech wood and then with PICA, allowing for a rare comparison between models used in different industrial sectors. In addition, a characterisation of the anisotropy and a parametric temperature study on these materials was also envisaged.

In a first step, the pyrolysis of a beech sample was carried out and the experimental data showed that the rate of devolatilization accelerated at the end of the pyrolysis due to a splitting of the sample and exothermic reactions. But it was not sufficient and data needed to be enriched before starting the pyrolysis of a PICA sample. In order to obtain such data, modifications to the experimental appartus were detailed.

During the 5 experiments performed, overheating, short circuits, and signs of loss of one-dimensionality occurred. The overheating and short circuits that cause a loss of longevity and quality of the experimental results were investigated to determine the cause. The problem was the design of the heat source, which was improved between each experiment but still has flaws. An improvement to the design was also proposed at the end of the experiments to ensure better one-dimensionality.

In order to carry out these experiments, a test bench was set up based on a version proposed in the plans last year and improved this year. In particular, the reactor was changed to be opened from the top to facilitate the reloading of biomass samples. In addition, a risk analysis and user manual had to be developed to ensure that the test bed could be operated safely.

In order to have a solid basis for evaluating the results of this study, the relevant scientific literature was synthesised. Large particle reactors similar to the one in this experiment were presented to give different design examples. The structure of the majority of pyrolysis models was developed to understand the usefulness of the one-dimensionality of the experiments and the assumptions and scope of the models. Results from TGA experiments were presented and parametric studies highlighted the influence of particle size, heating rate on devolatilization and temperature profile. In addition, the expected results for slow and fast pyrolysis were detailed as well as some transient heat transfer effects.

Some knowledge necessary for the understanding of this scientific literature was also introduced. Different ways of characterising wood were presented, as well as the pyrolysis of lignocellulosic biomass and its main aspects, such as mass and heat transfer, sample shrinkage, internal pressure generation, secondary reactions and products yield.

In conclusion, the high stakes of pyrolysis in the energy, chemical and aerospace industries have motivated the development of this experiment. The test bench has been designed, set up, tested and is not yet satisfactory in terms of results so some changes still need to be made to ensure longevity and data quality.

Appendix A

Design of the reactor

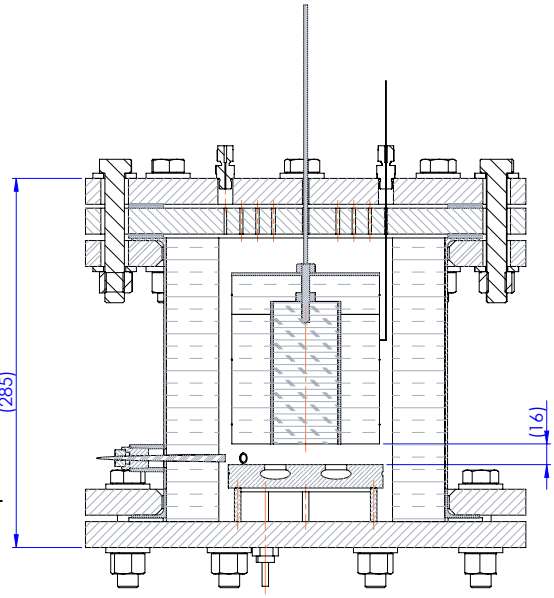

COUPE V-V
ECHELLE 1 : 3

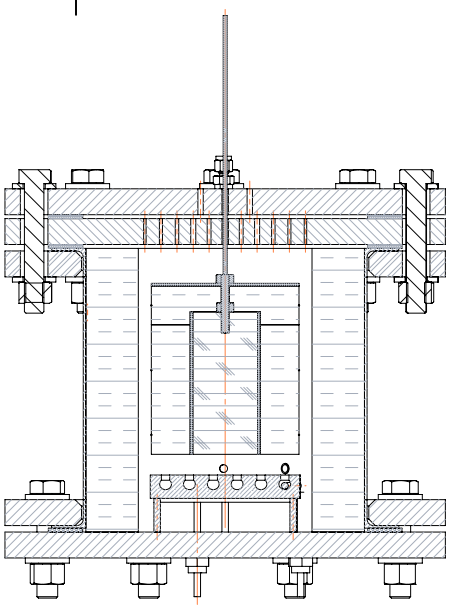

COUPE U-U
ECHELLE 1 : 3

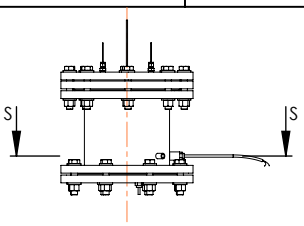

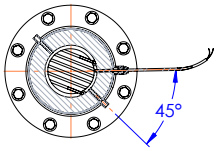

COUPE S-S

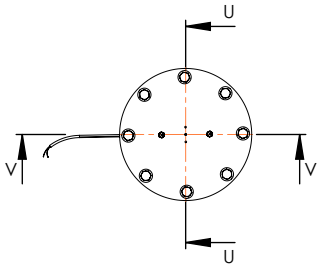

				Tolérance:	Etat de surface:
Auteur: Arnaud Lion	Date: 22-04-20	Rév:		Projet: Projet	
Matériau:					
Masse: 62124.38 gr				Description: Banc Pyrolyse	
UCLouvain Conception, Réalisation et Essais de Dispositifs ElectroMécaniques Institute of Mechanics, Materials, and Civil Engineering Place du levant, 2 bte L5.04.03 B-1348 Louvain-la-Neuve				Référence:	
				No. de plan:	
				Echelle: 1:10	Feuille: 1/2	Format: A3

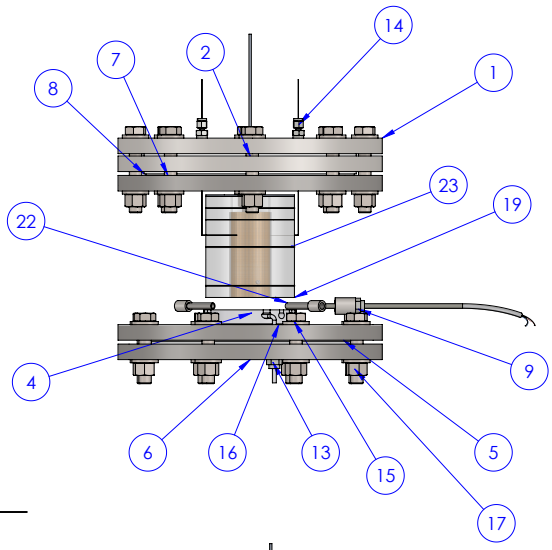

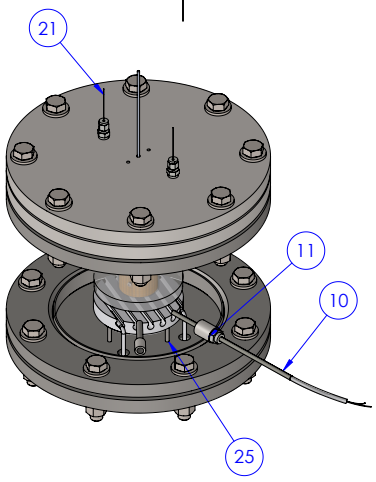

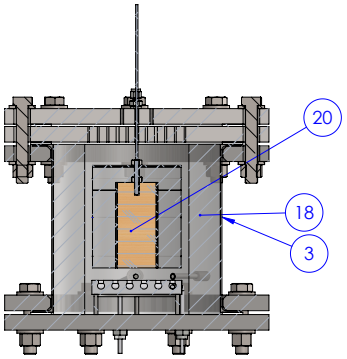

COUPE W-W

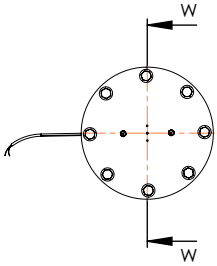

No. ARTICLE	NUMERO DE PIECE	DESCRIPTION	QTE
1	Bride DN200 - usinée	Bride Ø 300	1
2	Bride DN200 usinée - 2	Bride Ø300	1
3	Enveloppe extérieur	Tube DN 200	1
4	Dalle céramique avec fil	Description	1
5	Bride DN 200		2
6	Bride DN 200 pleine-usinée -1		1
7	collet DN200		2
8	Joint DN200 Graphite	Description	3
9	Raccord sonde temp 3-8	Description	1
10	Sonde température	Description	1
11	Manchon inox 3-8	Description	1
13	Raccord sonde temp 3-8.stp	Description	2
14	presse étoupe 1-8 G.stp	Description	2
15	DIN EN 24016 - M16 x 100 x 38-WN		16
16	Washer ISO 7415 - 16		32
17	ISO - 4033 - M16 - W - N		16
18	Fibre céramique extérieur	Description	1
19	Assemblage Cable Echantillon		1
20	Echantillon	Description	1
21	Thermocouple		2
22	Tube de sortie	Tube sortie Gaz	2
23	Fil serrage fibre céramique	Description	3
24	Tapping Screw ISO 14585 - ST2.9 x 6.5-C-N		2
25	Support Dalle céramique		1

Auteur: Arnaud Lion | Date: 22-04-20 | Rév:
Matériau:
Masse: 62124.38 gr

Tolérance: | Etat de surface:
Projet: Projet
Description: Banc Pyrolyse
Référence:
No. de plan:
Echelle: 1:4 | Feuille: 2/2 | Format: A3

UCLouvain
Conception, Réalisation et Essais de Dispositifs ElectroMécaniques
Institute of Mechanics, Materials, and Civil Engineering
Place du levant, 2 bte L5.04.03 B-1348 Louvain-la-Neuve

Appendix B

Piping and instrumentation diagram

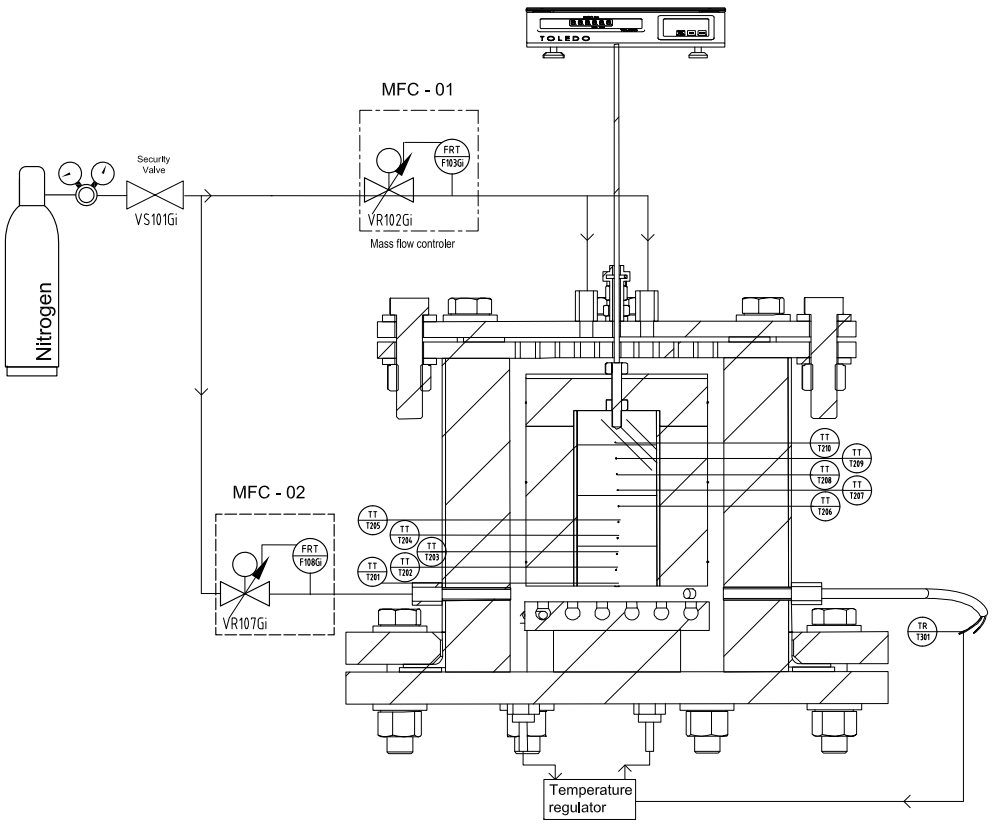

UCL Université catholique de Louvain	PROJET: TFE Pyrolyse SUBPROJECT: DESCRIPTION :	Remarque(s) : Jérémy de Visscher Dimitri Grevesse Resp : Designer : Date :
iMMC-TFL- place du Levant, 2 - B1348 - Louvain-la-Neuve Belgique Tél. +32(0)10-47.22.00 ; Fax. ++32(0)10-45.26.92; http ://www.uclouvain.be/immc	N° du dessin	Rev / Sheet. 1/1

REALISE A L'AIDE D'UN PRODUIT AUTODESK VERSION ETUDIANT

GR	IDEN.	NUM	REF.	DEFINITION	REMARQUE	Contained fluid
1	VS	101	V101Gi	soupape de sécurité		Azote
1	VR	102	V102Gi	vanne commandée régulation débit principal	6,5 Nl/min	Azote
1	FRT	103	F103Gi	débitmètre massique thermique		Azote
1	VR	107	F107Gi	vanne commandée régulation débit	1,4 Nl/min	Azote
1	FRT	108	F107Gi	débitmètre massique thermique		Azote
2	TT	201	T201	température surface échantillon	r = 0, z = 10	
2	TT	202	T202	température au centre de l'échantillon	r = 0, z = 9	
2	TT	203	T203	température au centre de l'échantillon	r = 0, z = 8	
2	TT	204	T204	température au centre de l'échantillon	r = 0, z = 7	
2	TT	205	T205	température au centre de l'échantillon	r = 0, z = 6	
2	TT	206	T206	température au centre de l'échantillon	r = 0, z = 5	
2	TT	207	T207	température au centre de l'échantillon	r = 0, z = 4	
2	TT	208	T208	température au centre de l'échantillon	r = 0, z = 3	
2	TT	209	T209	température au centre de l'échantillon	r = 0, z = 2	
2	TT	210	T210	température au centre de l'échantillon	r = 0, z = 1	
3	TR	301	T301	température source de chaleur		

Appendix C

User manual and Risk analysis

C.1 User manual

C.1.1 Principe de fonctionnement du pilote

Une résistance chauffante chauffe un échantillon de bois sous une atmosphère inerte d'azote. L'échantillon de bois se pyrolyse, c'est-à-dire que la matière volatile dont il est constitué s'évapore au fur et à mesure que la chaleur se propage dedans. L'azote injecté dans le réacteur a pour rôle de chasser et refroidir ces gaz de pyrolyse. Il provient d'une bonbonne placée à proximité du banc d'essai. L'intérieur du réacteur monte en température et est isolé de l'extérieur par des isolants thermiques. Les gaz de pyrolyse sont rejetés directement à l'extérieur du laboratoire via un tuyaux d'évacuation. Le but de l'expérience est d'obtenir l'évolution de la masse de l'échantillon de bois pyrolysé ainsi que la température à différents endroits de l'échantillon.

C.1.2 Mise en marche du pilote

Préalables

1. S'assurer que la zone de travail est dégagée, rangée et nettoyée de manière à pouvoir y circuler sans encombre.
2. Mettre l'équipement de protection individuel (EPI) constitué de : lunettes de sécurité, gants thermiques, chaussures de sécurité et tablier de laboratoire.
3. Vérifier la température extérieure du réacteur à l'aide des thermocouples.
4. Vérifier que l'alimentation de la résistance chauffante est débranchée.
5. Vérifier que la balance est sur son socle au dessus du couvercle du réacteur et que ses câbles d'alimentation et USB sont débranchés.
6. Vérifier que le tuyaux de sortie des gaz est retiré du réacteur.
7. Inspecter l'ensemble du banc d'essai pour s'assurer qu'il n'y a pas de défaut ni de dommage apparent.
8. Vérifier qu'il n'y a pas d'échantillon dans la gaine métallique et qu'elle est vide.
9. Vérifier que la vanne de sécurité est fermée.

Démarrage du pilote

1. Installer le nouvel échantillon dans la gaine métallique.
2. Tourner la table supportant le réacteur d'environ 30° par rapport au mur. Schéma ci-dessous

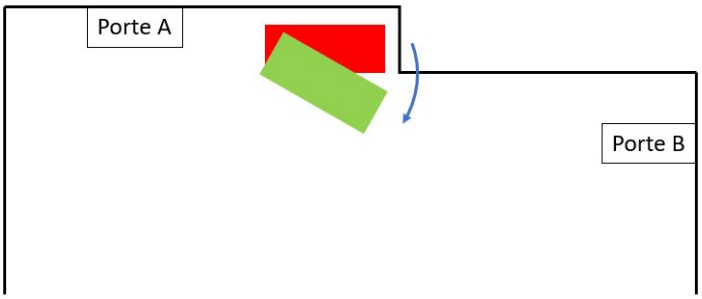

Figure C.1

3. Installer la sangle sur les anneaux du couvercle du réacteur et vérifier qu'elle y est correctement vissée.
4. Amener la grue d'atelier la monter à la hauteur adéquate et amener son crochet au dessus de la sangle. **Attention à bien rester en dehors de l'aire de travail de la grue d'atelier délimité par ses pieds.**
5. Insérer la sangle dans le crochet de la grue d'atelier et vérifier que le crochet est bien fermé.
6. Mettre en tension verticale la sangle avec la grue d'atelier.
   Remarque : Vérifier d'être 2 personnes minimum pour les opérations pendant lesquelles le couvercle du réacteur est en suspension afin de stabiliser le couvercle et le maintenir droit.
7. Lever le couvercle à bonne hauteur, en le maintenant droit.
8. Insérer la partie supérieure du câble de pesée dans le crochet de la balance (par-dessous son socle).
9. Glisser la partie inférieure du câble de pesée au travers du couvercle et la visser à la partie supérieure du câble à l'aide de l'écrou prévu à cet effet.
10. Insérer les thermocouples au travers du couvercle et puis dans l'échantillon via les trous prévus à cet effet au travers de la gaine métallique.
11. Envelopper la gaine métallique avec l'isolation et la serrer à l'aide d'un fil métallique.
12. Si nécessaire, déplacer la grue d'atelier pour amener le couvercle au dessus du réacteur.
13. Descendre le couvercle jusqu'à le poser sur le dessus du réacteur. Vérifier que le joint y est bien installé et pressé. **Attention, lors de cette étape il faut manipuler avec précaution la grue et le couvercle du réacteur pour éviter tout risque de pincement.**
14. Enlever la sangle.
15. Insérer le tuyau de sortie des gaz jusqu'à la marque adéquate et serrer ce même tuyaux pour qu'il soit fixé solidement.

16. Serrer la bride supérieure à l'aide des 8 écrous prévus à cet effet.
17. Brancher l'alimentation de la balance, l'allumer, la mettre à niveau et la connecter au PC du banc d'essai.
18. Vérifier la pression à la bonbonne d'azote, l'ouvrir et ouvrir doucement le détenteur jusqu'à obtenir une pression de 1.5 [bar].
19. Ouvrir la vanne de sécurité, et régler les débit des rota-mètres.
20. Lancer l'enregistrement des systèmes d'acquisitions de données (masse et température).
21. Brancher l'alimentation de la résistance chauffante.
22. Allumer la résistance chauffante avec une consigne de 800°C.

C.1.3 Fin d'utilisation de l'installation

Arrêt du pilote

1. Sauvegarder les enregistrements des données. **Attention à garder les mesures de températures activées, même sans les enregistrer.**
2. Arrêter l'alimentation de la résistance chauffante.
3. Débrancher l'alimentation du PID de régulation de la résistance chauffante.
4. Mettre hors tension la balance après l'avoir éteinte.
5. Attendre que toutes les températures baissent en dessous de 35°C avant de manipuler quoique ce soit sur le banc d'essai. **Etape qui peut prendre un certain temps, maintenir le flux d'azote.**
6. Fermer le détendeur de la bonbonne d'azote.
7. Fermer la vanne d'ouverture de la bonbonne d'azote.

Vidange de l'installation

1. Vérifier que tout soit à l'arrêt (voir section C.1.3), en particulier que les températures soient bien descendues en dessous de 35°C.
2. Débrancher les câbles d'alimentation et USB de la balance.
3. Retirer le tuyaux de sortie des gaz.
4. Tourner la table supportant le réacteur d'environ 30° par rapport au mur (cfr. figure C.1).
5. Desserrer et retirer les écrous qui maintiennent la bride supérieur. Déposer la bride supérieur sur les vis du bas.
6. Installer la sangle sur les anneaux du couvercle du réacteur et vérifier qu'elle y est correctement vissée.
7. Amener la grue d'atelier, la monter à la hauteur adéquate et amener son crochet au dessus de la sangle. **Attention à bien rester en dehors de l'aire de travail de la grue d'atelier délimité par ses pieds.**

8. Insérer la sangle dans le crochet de la grue d'atelier et vérifier que le crochet est bien fermé.
9. Mettre en tension verticale la sangle avec la grue d'atelier.
   Remarque : Vérifier d'être 2 personnes minimum pour les opérations pendant lesquelles le couvercle du réacteur est en suspension afin de stabiliser le couvercle et le maintenir droit.
10. Lever le couvercle à bonne hauteur, en le maintenant droit.
11. Retirer l'isolation autour de la gaine métallique.
12. Retirer les thermocouples insérés dans l'échantillon.
13. Dévisser la partie inférieur du câble de pesée afin de l'écrou prévu à cet effet afin de pouvoir manipuler aisément la gaine métallique contenant l'échantillon.
14. Dévisser l'échantillon et tout résidu solide de bois présent dans la gaine métallique.
15. Nettoyer la gaine métallique si nécessaire (résidu solide persistant,etc.).
16. Déposer délicatement le couvercle du récateur à l'aide de la grue d'atelier.
17. Mettre hors tension les appareils de mesure restant et le PC du laboratoire.

Précautions finales

1. Après avoir procédé à l'arrêt du pilote et à sa "vidange",
2. Vérifier que tous les appareils et l'équipement est hors tension.
3. Nettoyer tout déchet provenant de l'expérience, que ça soit sur le sol, sur la table, sur le banc d'essais, etc.
4. Signaler toute anomalie constatée dans le "carnet des utilisateurs". En informer l'équipe technique et/ou le responsable de l'installation.
5. Se laver soigneusement les mains.

C.2 Risk analysis : Kinnley method

Analyse de risque						Evolution des risques			
	Probabilité d'occurrence d'un accident	Fréquence d'exposition	Gravité de l'accident	Criticité	Prévention	Probabilité d'occurrence d'un accident	Fréquence d'exposition	Gravité de l'accident	Criticité
	0,1 à 10	0,5 à 10	1 à 100	0,05 à 10000		0,1 à 10	0,5 à 10	1 à 100	0,05 à 10000
Alimentation en azote					**Alimentation en azote**				
Montée en pression dans la conduite si conduits d'entrée dans le réacteur sont obstrués. Risque: conduite qui lache	0,2	6	7	8,4		0,2	6	7	8,4
Fuite à la bonbonne (surplus d'azote dans l'air) Risque: hypoxie	0,5	10	7	35	Vérification d'étanchéité	0,2	10	7	14
Fuite aux raccords ou dans la conduite d'entrée du réacteur Risque : hypoxie	1	10	7	70	Vérification d'étanchéité Débit faible (7.9L/min) et vérification du débit.	0,2	10	1	2
Banc d'essai					**Banc d'essai**				
Pièces chaudes Risques: Brûlures, incendie	6	6	7	252	Protocole d'utilisation strict Port d'équipements de protection individuel Pictogrammes Périmètre de sécurité autour du réacteur Isolant thermique supplémentaire (paroi du réacteur et conduite de sortie)	1	6	3	18
Présence de gaz inflammables dans les gaz de sortie Risque : intoxication, incendie, explosion, brûlures	2	6	7	84	Conduits étanches jusqu'à l'évacuation Forte dilution à la sortie de la cheminée Refroidissement du gaz de sortie avant éjection dans l'air	0,2	6	7	8,4
Surchauffe de composants Risque : 'incendie	1	6	15	90	Support du réacteur calorifuge (ajout d'une couche d'isolant thermique entre le réacteur et la table). Sonde de température pour résistante chauffante.	0,2	6	15	18
Chute du réacteur (objet contondant/tranchant) Risque : blessure	0,2	10	7	14	Périmètre de sécurité autour du réacteur Socle stable Port des EPI	0,1	10	7	7
Electricité					**Electricité**				
Risques d'électrocution	3	6	7	126	Formation des techniciens Pictogrammes de sécurité Mise à la terre du banc d'essai Protocole d'utilisation strict	0,2	6	7	8,4
Acoustique					**Acoustique**				
Nuisances sonores inexistantes/faibles	0,2	6	1	1,2		0,2	6	1	1,2
Risque matériel					**Risque matériel**				
Pièce chauffante surchauffe Risque: dégradation/destruction de composants	1	6	7	42	Sonde de température pour éviter de dépasser une température maximale, régulation en boucle courte via régulateur PID. Protocole d'utilisation strict	0,2	6	3	3,6

Bibliography

[1] Mottiat, Gilles ; Benoit, Julien. Development of a reference one-dimensional pyrolysis experiment. Ecole polytechnique de Louvain, Université catholique de Louvain, 2020. Prom. : Jeanmart, Hervé. http://hdl.handle.net/2078.1/thesis:25201

[2] G. Gauthier. "Synthèse de biocarburants de deuxième génération : étude de la pyrolyse à haute température de particules de bois centimétriques". PhD thesis. Ecole des mines d'Alibi-Carmaux, Dec. 2013. URL: https://tel.archivesouvertes.fr/tel-00999283

[3] V. Dhyani, T. Bhaskar. "Pyrolysis of Biomass, chapter 9"

[4] A. Hornung, Thermochemical Conversion of Biomass, 2014. https://dx.doi.org/10.1002/9781118693643.

[5] Bridgwater, A. V. Pyrolysis of biomass. In Biomass Power for the World: Transformations to Effective Use; Pan Stanford Publishing Pte. Ltd., 2015; pp 473-513

[6] Chan, W. C. R. Analysis of Chemical and Physical Processes During the Pyrolysis of Large Biomass Pellets. Ph.D. Thesis, University of Washington, Seattle, WA, 1983.

[7] Chan, W. C. R.; Kelbon, M.; Krieger-Brockett, B. Modelling and Experimental Verification of Physical and Chemical Processes during Pyrolysis of a Large Biomass Particle. Fuel 1985, 64, 1505-1513.

[8] Lai, W.-C. Reaction Engineering of Heterogeneous Feeds: Municipal Solid Waste as a Model. Ph.D. Thesis, University of Washington, Seattle, WA, 1991.

[9] Morten Gunnar Gronli. "A Theoritical and Experimental Study of the Thermal Degradation of Biomass". PhD thesis. The Norwegian University of Science and Technology, Nov. 1996.

[10] Shurong Wang et al. "Lignocellulosic biomass pyrolysis mechanism: A stateof-the-art review". In: Progress in Energy and Combustion Science 62 (2017), pp. 33 –86. DOI: 10.1016/j.pecs.2017.05.004. URL:http://www.sciencedirect.com/science/article/pii/S0360128517300266.

[11] T.R. Nunn et al. "Product composition and kinetics in the rapid pyrolysis of milled wood lignin". In: Industrial and Engineering Chemistry Process Design and Development 24.3 (Mar. 1985), pp. 836–844. DOI: 10.1021/i200030a053.

[12] Ali Akhtar, Vladimir Krepl, and Tatiana Ivanova. "A Combined Overview of Combustion, Pyrolysis, and Gasification of Biomass". In: Energy & Fuels 32.7 (2018), pp. 7294–7318. DOI: 10.1021/acs.energyfuels.8b01678.

[13] A. Demirbas. "Pyrolysis of ground beech wood in irregular heating rate conditions". In: Journal of Analytical and Applied Pyrolysis 73 (Mar. 2005), pp. 39– 43. URL:https://www.sciencedirect.com/science/article/abs/pii/S0165237004000889.

[14] L. Chen et al. “Influence of Particle Size, Reactor Temperature and Gas Phase Reactions on Fast Pyrolysis of Beech Wood”. In: International Journal of Chemical Reactor Engineering 8 (Apr. 2010).

[15] Colomba Di Blasi et al. “Pyrolytic behavior and products of some wood varieties”. In: Combustion and Flame 124.1 (2001), pp. 165 –177. DOI: 10.1016/ S0010-2180(00)00191-7. URL: http://www.sciencedirect.com/science/article/pii/S0010218000001917.

[16] R. Miller and J. Bellan. “A Generalized Biomass Pyrolysis Model Based on Superimposed Cellulose, Hemicellulose and Liqnin Kinetics”. In: Combustion Science and Technology - COMBUST SCI TECHNOL 126 (July 1997), pp. 97–137. DOI: 10.1080/00102209708935670

[17] D. Neves et al. “Characterization and prediction of biomass pyrolysis products”. In: Progress in Energy and Combustion Science 37 (Feb. 2011), pp. 611–630. DOI: 10.1016/j.pecs.2011.01.001.

[18] A. W. Coats and J. P. Redfern. “Thermogravimetric analysis. A review”. In: Analyst 88 (1053 1963), pp. 906–924. DOI: 10.1039/AN9638800906. URL: http://dx.doi.org/10.1039/AN9638800906.

[19] Julien Blondeau. “Investigation of pulverised biomass combustion: detailed modelling of particle pyrolysis and experimental analysis of ash deposition”. PhD thesis. Université catholique de Louvain - IMMC, May 2013. URL: http: //hdl.handle.net/2078.1/132579.

[20] R.A. Khalil et al. “Thermal analysis of energy crops: Part I: The applicability of a macro-thermobalance for biomass studies”. In: Journal of Analytical and Applied Pyrolysis 81.1 (2008), pp. 52 –59. DOI: 10 . 1016 / j . jaap . 2007 . 08 . 004. URL:http://www.sciencedirect.com/science/article/pii/S0165237007001350.

[21] Michaël Becidan, Øyvind Skreiberg, and Johan Hustad. “Products Distribution and Gas Release in Pyrolysis of Thermally Thick Biomass Residues Samples”. In: Journal of Analytical and Applied Pyrolysis - J ANAL APPL PYROL 78 (Jan. 2007), pp. 207–213. DOI: 10.1016/j.jaap.2006.07.002

[22] Hong Lu. “Experimental and Modeling Investigations of Biomass Particle Combustion”. PhD thesis. Ira A. Fulton College of Engineering and Technology; Chemical Engineering Department, 2006. URL: https://scholarsarchive.byu.edu/etd/778.

[23] Michel Bellais. “Modelling of the pyrolysis of large wood particles”. PhD thesis. KTH - Royal Institute of Technology, 2007.

[24] J. Larfeldt, B. Leckner, M.C. Melaaen. Modelling and measurements of the pyrolysis of large wood particles. In : Fuel 79 (2000) pp. 1637–1643 DOI : 0016-2361/00/$

[25] H. Lu et al. “Effects of particle shape and size on devolatilization of biomass particle”. In: 89.5 (2010), pp. 1156–1168. DOI: 10.1016/j.fuel.2008.10.023.

[26] Maschio, G., Lucchesi, A. and Koufopanos, C. A. (1994) Study of kinetic and transfer phenomena in the pyrolysis of biomass particles. In : A.V. Bridgwater,editor,Advances in Thermochemical Biomass Conversion, 2, pp. 746-759. Blackier Academic and Professional, New York

[27] E. Ranzi, A. Cuoci, T. Faravelli, A. Frassoldati, G. Migliavacca, S. Pierucci, and S. Sommariva. Chemical kinetics of biomass pyrolysis. Energy and Fuel, 22:4292–4300, 2008

[28] Oskar Paris, Cordt Zollfrank and Gerald A. Zickler. Decomposition and carbonisation of wood biopolymers—a microstructural study of softwood pyrolysis. In : Carbon 43 (2005), pp. 53-66 DOI: 10.1016/j.carbon.2004.08.034

[29] Williams, P. T.; Besler, S. Renewable Energy 1996, 7 (3), 233– 250.

[30] Santiago Septien, Sylvie Valin, Capucine Dupont, Marine Peyrot, Sylvain Salvador. Effect of particle size and temperature on woody biomass fast pyrolysis at high temperature (1000-1400 degrees C). Fuel, Elsevier, 2012, 97, pp.202-210. 10.1016/j.fuel.2012.01.049. hal-0168840

[31] Anup Kumar Sadhukhan, Parthapratim Gupta and Ranajit Kumar Saha. Modelling of pyrolysis of large wood particle. In : Bioresource Technology 100 (2009) pp. 3134–3139 DOI:10.1016/j.biortech.2009.01.007

[32] Van de Velden, M., Fan, X., Ingram, A., Baeyens, J., 2007. Fast pyrolysis of biomass in a circulating fluidised bed. In: Berruti, F., Bi, X., Pugsley, T. (Eds.), Twelfth International Conference on Fluidization – New Horizons in Fluidization Engineering Fluidization XII. Vancouver, Canada, pp. 897–904.

[33] R. Bilbao et al., Modelling of the pyrolysis of wet wood, Journal of Analytical and Applied Pyrolysis 36 (1) (1996) 81–97.

[34] C.A. Koufopanos et al., Modelling of the pyrolysis of biomass particles. Studies on kinetics, thermal and heat transfer effects, Canadian Journal of Chemical Engineering 69 (4) (1991) 907–915.

[35] V. Strezov, B. Moghtaderi, J. Lucas, Thermal study of decomposition of selected biomass samples, Journal of Thermal Analysis and Calorimetry 72 (3) (2003) 1041–1048.

[36] Won Chan Park, Arvind Atreya, and Howard Baum. "Experimental and theoretical investigation of heat and mass transfer processes during wood pyrolysis". In: Combustion and Flame 157 (Mar. 2010), pp. 481–494. DOI: 10.1016/j. combustflame.2009.10.006.

[37] Park, Y., Kim, J., Kim, S., Park, Y.K., 2009. Pyrolysis characteristics and kinetics of oak trees using thermogravimetric analyzer and micro-tubing reactor. Bioresource Technology 100, 400–405.

[38] D. L. PYLE and C. A. ZAROR. Heat transfer and kinetics in the low temperature pyrolysis of solids. In : Chemical Engineering Science Vol. 39, No. 1,pp. 147-158, 1984. DOI : 0009-2509/84

[39] Munir, S., Daood, S.S., Nimmo, W., Cunliffe, A.M., Gibbs, B.M., 2009. Thermal analysis and devolatilization kinetics of cotton stalk, sugar cane, bagasse and shea meal under nitrogen and air atmospheres. Bioresource Technology 100, 1413–1418.

[40] Cuoci, A. T.; Faravelli, A.; Frassoldati, S.; Granata, G.; Migliavacca, E.; Ranzi, S.; Sommariva, A. General Mathematical Model of Biomass Devolatilization, 30th Meeting of the Italian Section of the Combustion Institute; 2007

[41] P.O. Okekunle et al. "Numerical and experimental investigation of intra-particle heat transfer and tar decomposition during pyrolysis of wood biomass". In: Journal of Thermal Science and Technology 6.3 (Apr. 2011), pp. 360–375. DOI: 10. 1299/jtst.6.360.

[42] P.O. Okekunle et al. "Effect of biomass size and aspect ratio on intra-particle tar decomposition during wood cylinder pyrolysis". In: Journal of Thermal Science and Technology 7.1 (Oct. 2012), pp. 1–15. DOI: 10.1299/jtst.7.1.

[43] H. Rezaei et al. "A numerical and experimental study on fast pyrolysis of single woody biomass particles". In: Applied Energy 198 (2017), pp. 320–331. DOI: 10.1016/j.apenergy.2016.11.032.

[44] Wen-guang Wu et al. "Isothermal Pyrolysis of Biomass by Macro-TG". In: AsiaPacific Power and Energy Engineering Conference, APPEEC (Mar. 2009). DOI: 10. 1109/APPEEC.2009.4918456.

UNIVERSITÉ CATHOLIQUE DE LOUVAIN
École polytechnique de Louvain
Rue Archimède, 1 bte L6.11.01, 1348 Louvain-la-Neuve, Belgique | **www.uclouvain.be/epl**